(810)

" DESIGN AND FABRICATION OF A POLARIZATION TRANSFORMER FOR THE MEASUREMENT OF HELICITY OF BETA PARTICLES USING MOTT SCATTERING "

Thesis for the Degree of Doctor of Philosophy
in the Faculty of Engineering,
University of Indore,
I N D O R E

Submitted by
S.S. ABHYANKAR, M.Sc.

DEPARTMENT OF APPLIED PHYSICS,
Shri. G.S. Technological Institute,
INDORE UNIVERSITY, INDORE

ACKNOWLEDGEMENTS

I am deeply indebted to Dr. M.R. Bhiday, Ph.D.(Nag.), Ph.D.(London), A.Inst.P.(London), Professor and Head of the Department of Applied Physics, G.S. Technological Institute, Indore, for his keen interest and valuable guidance throughout the work.

I am equally grateful to Dr. S.M. Dasgupta, Principal, G.S. Technological Institute for encouragement and providing the necessary facilities, during the course of this investigation.

I am also thankful to Dr. A. Goswami, Head of the Electron Microscope Division National Chemical Laboratory, Poona, for providing the facilities for preparing the gold foils.

I am particularly thankful to Professor R. Steffen, University of Purdue, U.S.A. and to Dr. V.G. Kulkarni, Tata Institute of Fundamental Research for their willing and ready co-operation in supplying other literature on the subject and useful discussions.

My sincere thanks are due to Dr. K.G. Bhatnagar, Dr. D.V. Bhavalkar and Dr. P.K. Bhattacharya for their valuable guidance and help in the present work.

I am also thankful to Shree N.M. Chowdhary,

Shri K.W. Phadke, Shri R.C. Mahant, Dr. Sharda, Dr. Shastri and other colleagues, and also to other workers in this Laboratory and the workshop staff specially Prof. Banerjee, Workshop Superintendent for their help and co-operation.

I am also obliged to the University Grants Commission, New Delhi for the financial assistance given to this project under their research assistance programme to university teachers.

Dt. 18-2-1969.

S.S. Abhyankar.
(S.S. Abhyankar)

DEPARTMENT OF APPLIED PHYSICS,
Shri G.S. Technological Institute,
INDORE

C O N T E N T S

CHAPTER I

INTRODUCTION

I-1. Importance of Helicity Measurements:

Experiments involving the polarization of electrons and photons are important in two respects: First, they yield information about the basic properties of electrons and photons, such as 'g' factor of free electrons. Secondly, information gained from polarization experiments ties in closely with data from the decay of polarized nuclei, beta-gamma circular polarization correlations, beta-neutrino angular correlations, and neutrino helicity measurements.

It required considerable time and effort to show that photons possess the properties of massless particles with spin 1, and that free electrons display the polarization phenomena predicted by the Dirac theory for spin $\frac{1}{2}$ particles. Since these basic questions have been understood satisfactorily, one can use the polarization measurements to determine the 'g' factor of free electrons, and to investigate the properties of nuclear levels. The application of polarization measurements to problems connected with parity non-conservation is also of major importance.

Since 1956, the question whether the weak

interactions are invariant under spatial inversion($r \rightarrow -r$), charge conjugation, and time reversal was seriously considered.

In order to solve the θ-τ puzzle, Lee and Yang(1) undertook a systematic investigation of the validity of parity conservation. They found that parity is conserved to a high degree of accuracy in electromagnetic and strong interactions, but that the principle of parity conservation is "only an extrapolated hypothesis, unsupported by experimental evidence" for the weak interactions responsible for beta-decay as well as for the decay of all unstable particles (with the exception of π^- and Σ^0). They suggested several experiments that would test the principle of parity conservation for these weak processes. According to the underlying theory, spin S is a pseudovector and that experimentally observable terms like $\mathbf{S}.\hat{\mathbf{p}}$ (where $\hat{\mathbf{p}}$ is the unit vector in the direction of momentum) is a pseudoscalar under the parity operation, $\mathbf{r} \rightarrow -\mathbf{r}$, $\hat{\mathbf{p}}$ changes sign, while S does not. Hence, the helicity operator $P_\ell(p) = \mathbf{S}.\hat{\mathbf{p}}$ changes sign. If parity is conserved, the expectation value of P_ℓ must vanish. Thus, a non-vanishing expectation value demonstrates parity non-conservation.

The present experimental evidence is compatible with, and in fact, strongly favours, maximum parity violation in beta-decay. A particularly elegant formulation

in agreement with present experimentation is the two component neutrino theory, independently proposed by Landau(2), Lee and Yang(3) and Salam(4). As stated by Landau(5), rejection of the laws of conservation of parity entails the possibility of existence of new properties of the neutrino, i.e., longitudinal polarization.

According to experiment the decay operator should be represented as the sum of the scalar and tensor variants. It can be shown that in either case, the same electron polarization in the direction of motion will arise which can be shown equal to v/c (or - v/c). It is also consistent with time reversal invariance. The restrictions that these conditions impose on the strengths of the coupling constants are as follows:

(a) Time reversal invariance (under CPT theorem) requires that all coupling constants be real with respect to one another.

(b) The Lee and Yang two component neutrino theory requires that the parity conserving and non-conserving coupling constants be equal in magnitude.

$$C_i = C_i'$$

(c) The simplest conditions on the coupling

constant compatible with $P_\ell = \pm v/c$ are

$$C_S = C_T = C_p = 0 \quad \text{and} \quad \begin{matrix} C_A = C_A' \\ C_V = C_V' \end{matrix}$$

where C_S, C_V, C_T, C_A, C_p and C'_S, C'_V, C'_T, C'_A, C'_p corresponds to parity conserving and non-conserving coupling constants. More recently Feynman and Gell Mann(6) and Sudershan and Marshak(7) restricted the arbitrary mixture for coupling constants and in their symmetrization of the theory led to the unique V $\pm$ A form of the coupling, while, the S and T coupling are ruled out. This V $\pm$ A theory is universal for all weak interactions.

The allowed beta-decay $0^+ \text{—} 0^+$ is a pure Fermi transition. We know that the electron and the neutrino are emitted predominantly into the same hemisphere, and the antineutrino is right handed. Since the nuclear system initially had a total spin 0, the electron must have its spin opposite to its direction of motion, i.e., it must have negative helicity.

Asymmetry in the beta-emission from polarized nuclei also implies an electron polarization. Considering an allowed Gammo-Teller decay $1^+ \text{—} 0^+$, we know that the electrons are emitted predominantly opposite to the direction of the nuclear orientation. Angular momentum can then only be conserved if the electron has negative helicity.

While helicity experiments on allowed transitions help to elucidate the laws of beta-decay, investigations on forbidden transitions can give information about nuclear-matrix elements and perhaps also about time-reversal invariance and conserved vector current effects. In certain forbidden beta decays, such as RaE, the usually dominant matrix elements interfere destructively. The resulting spectrum shape can differ from the shape typical for the order of forbiddenness, and the electron polarization can be smaller than v/c.

An accurate knowledge of the energy dependence of the polarization in continuation with the spectrum shape allows the relative magnitude of several matrix elements to be fixed. The values of these matrix elements are expected to show the effects of a possible violation of time-reversal invariance in beta decay. The helicity of beta particles has been observed in a large number of cases. All allowed and most forbidden decays show within rather wide limits of errors a complete polarization ($P_p = \pm v/c$). The first exception to this rule was found by Geiger and Co-workers(8), who determined the helicity of electron from RaE and found it to be less than v/c. Experimentally such deviations have been observed in a number of decays(9-15).

I-2. Outline of the Proposed Work:

As stated in Section (I-1) the theory of beta

decay predicts that the degree of polarization should be proportional to v/c, and that deviations from full polarization have been reported by several workers. There is, as yet, no conclusive evidence on the manner in which polarization depends on the atomic number Z of the emitting nucleus. Similarly, the energy (momentum) dependence of polarization also needs a careful investigation. It was thought, therefore, necessary to study this aspect of helicity in some detail. With this end in view, the design and fabrication of the equipment was undertaken and the performance of the same is reported in this thesis.

It was decided to use the Mott-scattering of polarized electrons on gold foil of various thicknesses, for the measurement of helicity. The Mott-scattering was proposed to be studied in various azimuthal planes. It was, however, thought difficult to use the Mott-scattering method(16) for transforming the polarization of the beta particles incident on the foil.

It was, therefore, found necessary to use another polarization transformer, and the choice fell on the Wien-filter method(P. 39) (crossed electric and magnetic field arrangement), as discussed in detail, on page 28 Chapter II.-5 (iii)

I-3. Description of Polarization and Definition of Helicity:

In general, a particle with spin S possesses(2S+1) possible orientations of its intrinsic angular momentum, with respect to a given direction. A particle beam is called unpolarized if all of these states are equally populated for any choice of quantization axis. The electron, a particle with spin $\frac{1}{2}$, possesses two polarization states. If the direction of quantization is chosen along the direction of motion i.e., if spin and momentum are parallel or antiparallel, one talks about longitudinal polarization or "Helicity".

Because both electrons and photons possess two states of polarization, the formal description of the polarization is very similar. Further, that the longitudinal polarization (helicity) is to a large degree conserved in the various transformations involving photons and electrons is an important aspect. Thus, longitudinally polarized electrons give rise to circularly polarized photons in bremsstrahlung, and circularly polarized photons produce longitudinally polarized electrons in pair production and in the photo effect.

Electrons possess two polarization states, for any given direction Z, i.e., the spin can either be "up or down". Assume that one has defined Z by an experimental

arrangement and that one has determined the probability N (+) for finding electrons with spin "up and N (-) for finding electrons with spin "down", one then defines polarization:

$$P_z = \frac{N(+) - N(-)}{N(+) + N(-)} \quad \ldots\ldots\ldots \quad (1)$$

except for the case of complete polarization along z $[|P_z| = 1]$, such an experiment does not yield all the information that can be extracted from a given beam. For a complete description of the polarization, a measurement of the spin along three mutually orthogonal directions X, Y, and Z is required. The degree of polarization is then given by

$$P = \sqrt{P_x^2 + P_y^2 + P_z^2} \quad \ldots\ldots\ldots \quad (2)$$

where, P can vary between o and 1.

In order to connect the observationally defined polarization with theoretical results considering, non-relativistic electrons, if $\psi = \begin{pmatrix} \psi_1 \\ \psi_2 \end{pmatrix}$ is the normalized two-component wave function describing the electron, a polarization vector P is defined as the expectation value of the Pauli-spin operators $\sigma \equiv (\sigma_1, \sigma_2, \sigma_3)$.

$$P = (\psi, \sigma, \psi) = \langle \sigma \rangle$$

$$\sigma = \left\{ \begin{pmatrix} 0 & 1 \\ i & 0 \end{pmatrix}, \begin{pmatrix} 0 & -i \\ i & 0 \end{pmatrix}, \begin{pmatrix} 1 & 0 \\ 0 & -1 \end{pmatrix} \right\}$$

P transforms like a vector and it is legitimate to say that P points in the direction of the electron spin. Of particular interest is the longitudinal polarization or helicity P_ℓ, defined as the component of polarization along the direction of motion of the electron. P_ℓ is given by the expectation value of the operator $\sigma \cdot \hat{p} = \langle \sigma \cdot \hat{p} \rangle$ where, $\hat{p}$ is the unit vector in the direction of the momentum p. Values of $P_\ell = +1$ and -1, are for the two states denoted as right handed and left handed helicities.

For relativistic electrons, according to Dirac theory, spin and momentum are coupled and $P_\ell = \langle \overline{\sigma \text{ Dirac}} \cdot \hat{p} \rangle$ The probability that $\sigma \cdot p = +p$ is given by

$$\left| \psi (+) \right|^2 = 2 \left(\frac{W + m + p}{W + m} \right)^2$$

Similarly, the probability that $\sigma \cdot p = -p$ is given by

$$\left| \psi (-) \right|^2 = 2 \left(\frac{W + m - p}{W + m} \right)^2$$

the helicity P is then given by

$$P_\ell = \frac{|\psi(+)|^2 - |\psi(-)|^2}{|\psi(+)|^2 + |\psi(-)|^2} = \frac{p}{W} = V \left(v/c \right).$$

where, W is the total energy and P the momentum.

Considerable experimental work has been carried out to check the above theory. This is reviewed in

Chapter II. This will enable one to have proper appreciation of the difficulties in this work and also to understand the different salient features which need further experimentation.

CHAPTER II

REVIEW OF EARLIER WORK

II-1. Introduction:

The helicity of electrons has been measured by several workers using, Mott-scattering (e,n), Møller(e,e) scattering and Bremsstrahlung. Each of these interactions has been found useful in an energy range not covered by the other two.

Møller scattering (e,e) and Bhabha scattering ($\vec{e}^{+}$,e) involving scattering of $\vec{e}^{+}$ or $\vec{e}^{-}$ by polarized electrons in a ferromagnetic foil, are useful at low energies, but experimental difficulties at these energies have so far limited their application to the range from 300 to 1000 Kev.

The bremsstrahlung (Ec) cross section increases almost linearly with electron energy and helicity. Longitudinally polarized electrons produce circularly polarized bremsstrahlung. The degree of circular polarization is determined by scattering or transmission using magnetized foils of iron. Helicity measurements have so far been carried out at electron energies greater than about 1 Mev.

Mott scattering means scattering of electrons by the coulomb field of heavy nuclei. Mott(17) showed that this is spin dependant. The cross section as well as the polarization effect in Mott scattering is largest at low energies (·03-1 Mev). For both these reasons, Mott scattering measurements of polarization have been confined with few exceptions to electrons of energies below 500 Kev.

The Møller scattering and bremsstrauhlung methods are reviewed briefly in the following sections, in order to enable a proper evaluation of the Mott scattering method adopted in the present work.

II-2. Møller Scattering Methods:

The strong dependence of the electron-electron scattering cross section on the initial directions of polarization of the two electrons indicated the possibility of measuring the longitudinal polarization of electrons from beta decay by scattering from an iron target, (δ max foil or supermendur). In this system, the spins of the two ferromagnetic 3 d electrons have been aligned parallel or antiparallel to the direction of the incident (beta decay) electrons. The basic arrangement for the measurement of electron and positron helicity by means of Møller and Bhabha scattering is shown in fig.(1).

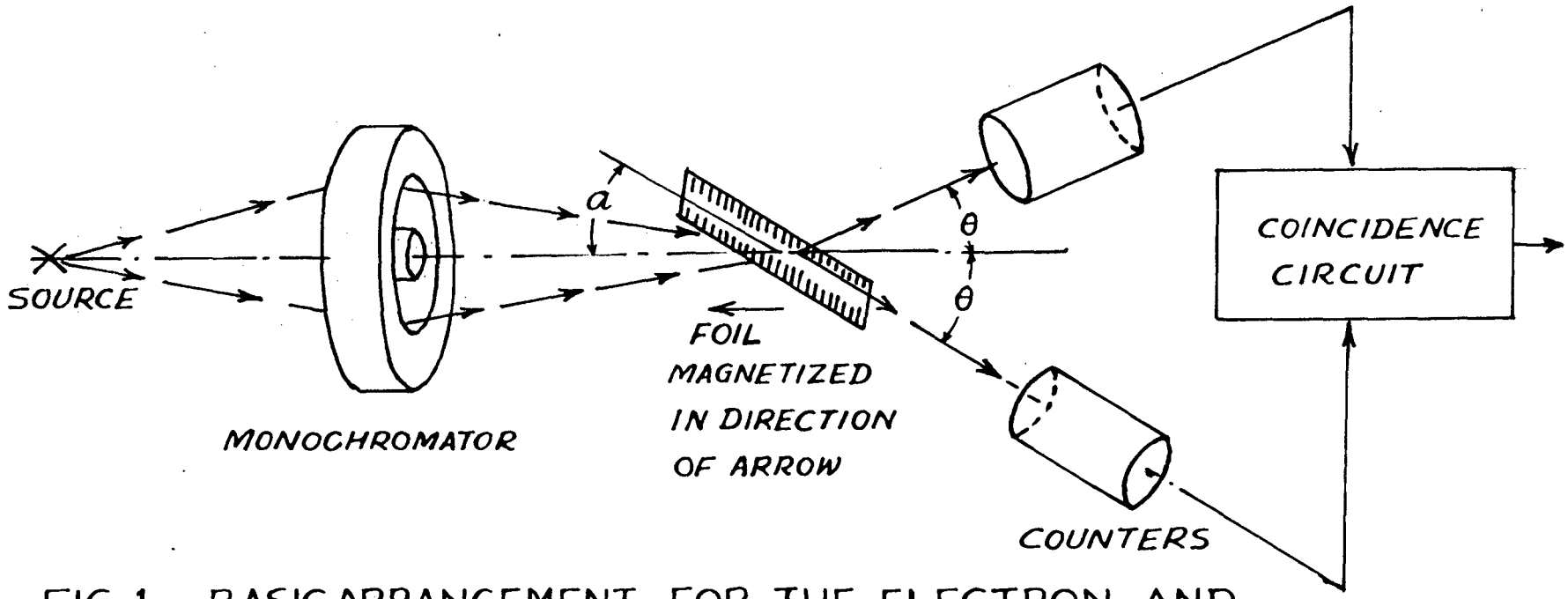

FIG. 1. BASIC ARRANGEMENT FOR THE ELECTRON AND POSITRON HELICITY MEASUREMENT BY MOLLER AND BHABHA SCATTERING

A ferromagnetic magnetized foil provides polarized target electrons, and coincidence counting is used to detect Møller collisions. The angle θ is the laboratory scattering angle corresponding to a 90^{o} C.M. scattering angle. A beta monochromator selects electrons in the desired momentum band. The Møller scattered electrons at 90^{o}C.M. scattering angle possess half the selected energy. Pulse height analysis, with slow-fast coincidence circuit of nano second resolving time, distinguishes the Møller scattered electrons from Mott scattered ones. Energy selection and coincidence arrangement together form a very effective means for separating out the desired events.

In practice, the method is used for the determination of longitudinal polarization. In this case the target electrons should be polarized in the direction of the incident electron beam. Unfortunately, extremely high fields are necessary to magnetize a thin foil in a direction normal to its surface. Therefore, it is necessary to magnetize the foil along its surface and incline it at an angle to the electron beam, as shown in fig.(1). If the fraction of electrons aligned in the foil is f , and the angle of inclination of the foil to the electron beam is α , the target electrons will have longitudinal polarization $f \cos \alpha$ when looked at in the

c.m. system. The relative change δ of the coincidence counting rate is defined as

$$\delta \equiv 2\left(C_p - C_a\right)\Big/\left(C_p + C_a\right).$$

where, C_p and C_a are numbers of coincidences when the incident electron momentum and the polarizing magnetic field in the scattering foil are parallel, and antiparallel, respectively.+

In terms of longitudinal polarization P of the incident electrons, δ is given by

$$\delta = 2f \cos\theta\, P\left(1-\xi\right)\Big/\left(1+\xi\right)$$

where, $\xi \equiv \phi_p/\phi_a$, is the ratio of the scattering cross sections for longitudinally polarized electrons with parallel and antiparallel spins as given by Bincer(18).

II-3. Bremsstrahlung Method:

The basic idea underlying the determination of the electron helicity by using the bremsstrahlung is to measure the polarization of the bremsstrahlung emitted in the radiator by the beta particle. The experimental arrangement of Lipnik et al(19), is shown schematically in fig.(2).

+ Actually, these directions are not exactly parallel and antiparallel to each other; the angle between them is θ and $180-\theta$.

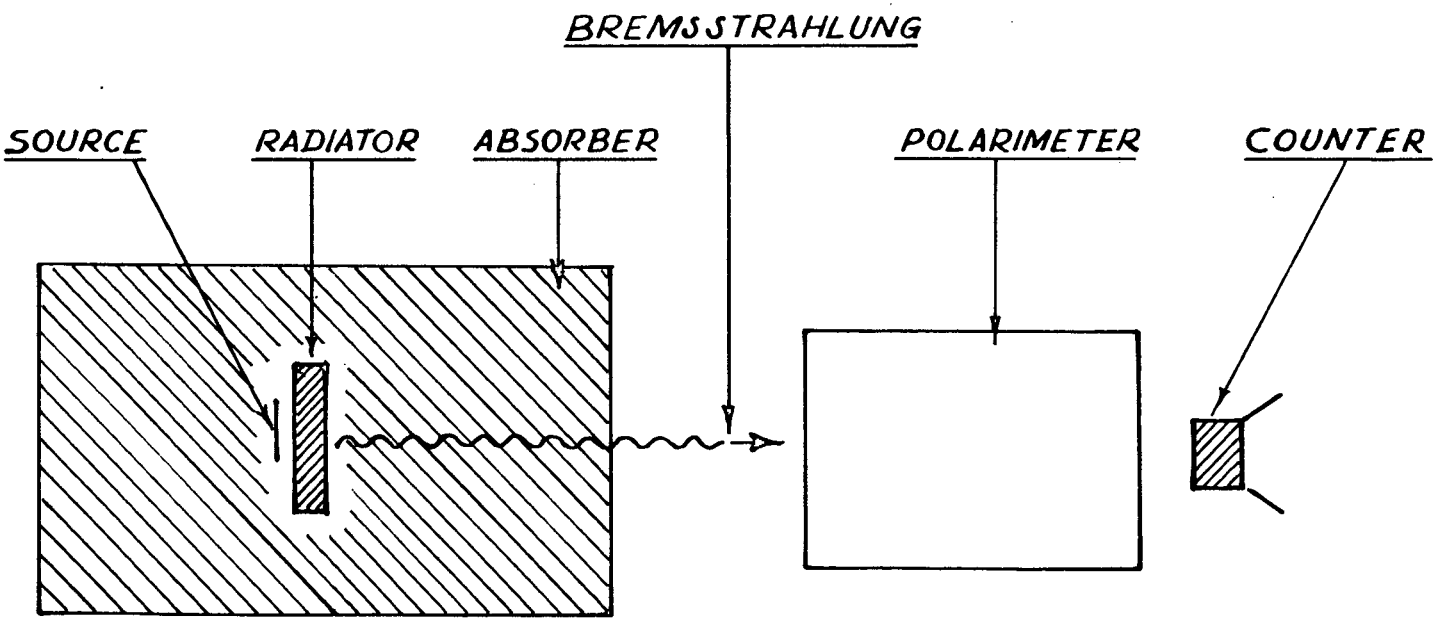

FIG. 2 EXPERIMENTAL ARRANGEMENT OF LIPNIK ETAL FOR HELICITY OF ELECTRONS BY BREMSSTRAHLUNG METHOD

The external bremsstrahlung is produced by an electron which leaves the nucleus and then radiates in the field of another nucleus. The intensity of the external bremsstrahlung is approximately proportional to the atomic number Z, of the radiator. The internal bremsstrahlung which originates in the atom of the decaying nucleus, is much weaker than the external bremsstrahlung and its intensity is approximately independent of the atomic number of the source. In the arrangement shown, the source will emit internal bremsstrahlung, and beta particles. The internal bremsstrahlung quanta are circularly polarized. The beta particles, give rise to circularly polarized external bremsstrahlung quanta in the radiator. The experimental set up must be so designed that (a) no electrons should give rise to bremsstrahlung originating in the polarimeter and the absorber should be of low Z; (b) separation between internal and external bremsstrahlung is achieved by measuring the bremsstrahlung intensity as a function of the atomic number Z.

For arbitrary polarization, characterized by a degree of polarization P and a polarization angle Φ, the circular polarization P_3 of the bremsstrahlung, is given by P_3 (photon) = P (L cos Φ + T sin Φ). The helicity of the bremsstrahlung is, thus, proportional to the degree

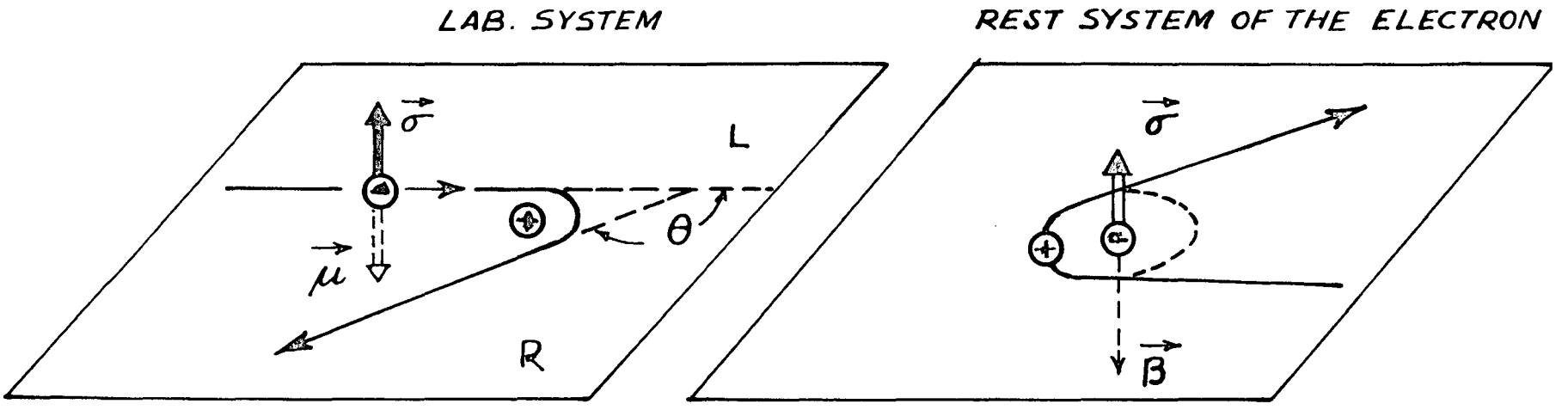

FIG. 3 BASIC PHYSICAL IDEA UNDERLYING MOTT SCATTERING

of polarization of the electrons, where L and T are the ratios of the photon helicity to electron helicity for longitudinal and transverse polarized electrons respectively.

II-4. Mott Scattering Method:

II-4(i) The basic physical idea underlying Mott scattering can be described with the aid of fig.(3). Assuming that an electron is scattered in a plane perpendicular to its spin, the existence of a spin orbit interaction is then easiest to see in the rest system of the electron, where, the nucleus moves around the electron. This motion gives rise to a magnetic field at the electron. If the magnetic field and the magnetic moment of the electron are parallel, the attractive potential is increased. This happens for electrons scattered to the right, and one expects increased scattering to this side. Electrons with spin "up" i.e. with magnetic moment down, approaching a nucleus of positive charge straight ahead, are predominantly scattered to the right.

In the laboratory system, the incident electron with spin σ perpendicular to the plane of scattering is deflected by an angle θ to the right. In the electron rest system, the nucleus orbits partially around the electron and creates a magnetic field B.

The result of this spin-orbit interaction is that

transversely polarized electrons will show a scattering pattern which is not symmetrical in the plane extended by the spin and momentum vectors of the incoming electrons. Thus, a system of two identical detectors placed symmetrically about the above mentioned plane will show different counting rates, the difference depending on the degree of polarization.

II-4(ii) For a quantitative description of the asymmetry in Mott scattering, we introduce the differential cross section ($d\sigma/d\Omega$) for an unpolarized beam and an asymmetry function S (θ, W, Z). The quantity S (θ, W Z) is the polarization produced, if an unpolarized electron beam of total energy W is scattered by a thin target of atomic number Z and θ is the scattering angle. Hereafter, the quantity S (θ, W, Z) will be written as S(θ).

To describe the Mott scattering of a polarized beam, we introduce spherical co-ordinates, with the Z axis along the momentum of the incident electron. The transverse polarization P of the incident electron shall lie along the azimuth Φ_0 and the scattering shall be described by a polar angle θ and an azimuthal angle Φ .

The cross section for Mott scattering can be written as

$$\frac{d\sigma}{d\Omega}\left(\theta,\ \Phi-\Phi_0\right) = \frac{d\sigma}{d\Omega}(\theta)\left[1 - P\,S(\theta)\,\sin\left(\Phi-\Phi_0\right)\right] \quad \cdots (4)$$

In general, the plane of scattering will be selected in such a way that the asymmetry becomes maximum. This occurs for scattering in the plane perpendicular to the polarization vector, where, $\Phi - \Phi_0 = 3\pi/2 \equiv -\pi/2$. for scattering to the right. "Left" is thus defined by a unit vector $\hat{L}$ such that $\hat{L} = \hat{P} \times \hat{p}$, where, $\hat{P}$ and $\hat{p}$ are unit vectors in the direction of the polarization and the momentum of the incident electron respectively.

The ratio of the intensities of electrons scattered to the left to electrons scattered to the right then becomes

$$\frac{L}{R} = \frac{\frac{d\sigma}{d\Omega}(\theta, -\pi/2)}{\frac{d\sigma}{d\Omega}(\theta, +\pi/2)} = \frac{1 + P S(\theta)}{1 - P S(\theta)} \quad \cdots (5)$$

The transverse polarization P is thus given by

$$P = \frac{L - R}{S(\theta)(L+R)} \quad \cdots \quad \cdots \quad (6)$$

II-4(iii) Measurement of polarization: In the electron polarization experiments the polarization to be measured is longitudinal. The Mott scattering pattern of a longitudinally polarized electron is symmetrical. Therefore, some sort of a spin twisting mechanism has to be applied to the electrons before scattering takes place in order to make use of the above mentioned scattering asymmetry.

The basic experimental set up for Mott scattering method is, therefore, simple. The beam of longitudinally polarized beta particles is first passed through a polarization transformer, where it is transformed to a transversely polarized beam, the degree of transformation depending upon the experimental conditions. This transformed beam then strikes the thin scattering foil of high Z value (usually of gold). A small fraction of electrons (10^{-4} - 10^{-5}) suffers a large angle scattering and enters one of the two symmetrically arranged counters, C_L or C_R. The ratio of L/R of the intensities in the two counters is a direct measure of the transverse polarization.

The most complete calculations of $d\sigma/d\Omega$ and of the asymmetry function $S(\theta)$ have been performed by Sherman(20). Lin and Percus(21) have performed these calculations taking screening effect into consideration for gold and mercury at a few values of energy.

II-4(iv) Correction to be applied: Theoretically this procedure of measurement of polarization is straightforward and simple. In practice, however, there exist considerable difficulties and the experimental ratio $(L/R)_{exp.}$ must be corrected for many possible deviations from an ideal set up, before a reliable value for the polarization P can be obtained. A few remarks concerning

the most important corrections are given below:

(a) Plural and multiple scattering in the target are the most important sources of error in Mott scattering. The contribution from multiple scattering can be calculated resonably well(22). The best method(23) to corredt for this error from plural and multiple scattering, consists in determining intensities L and R as a function of the target thickness and then extrapolating to zero thickness.

(b) Depolarization can occur in the source, the source backing material, the material between the source and the foil, and the foil itself. The magnitude of the depolarization is usually estimated with the help of theoretical calculations(24). Experimentally one can find some information by changing the various parts of a set up in a controllable manner(25).

(c) The source, the polarization analyzer, the target, and the counters subtend finite solid angles. The momentum selector also possesses a finite momentum resolution requiring corrections to be applied for these errors.

II-5. Review of the Previous Experimental Work on Mott-scattering:

The various experiments on the measurements of helicity of electrons using Mott scattering can be classified according to the methods used for transforming

the polarization from longitudinal to transverse one. These are (i) Double scattering methods, using Coloumb field of low Z material as a polarization transformer, (ii) Measurements using radial electrical field, such as in cylindrical or spherical condenser, and (iii) experiments using a crossed electric and magnetic field i.e. Wien filter arrangement.

II-5(i) Double scattering methods: DE SHALIT. S. Kuperman et al (26) have measured the longitudinal polarization of electrons from P^{32} by double scattering method. The electrons were first scattered through 90^{o} by a semicircular aluminium foil σ_1 (0.05 cm thick) which transforms the longitudinal polarization into a partial transverse polarization. The diameter of the semi-circle describing the foil is along the line joining the source to the other foil σ_2(2.5 mg/cm^2 Au), where the electrons undergo a second scattering for polarization analysis. The electrons which are scattered to the right and to the left by 75^{o} are recorded by two scintillation counters C_R and C_L.

The situation concerning the relative direction of the magnetic moment and the electron momentum is shown in fig(4) for the case of non-relativistic electrons. The electron is initially polarized with spin S in the direction opposite to its direction of motion. Since the

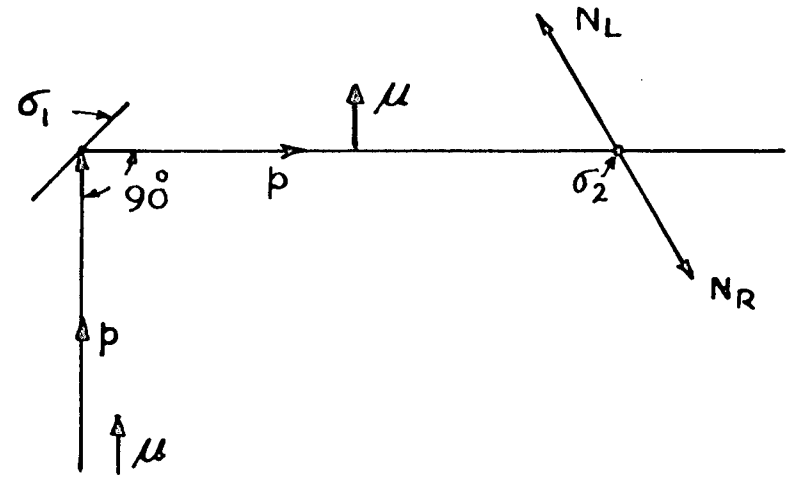

FIG. 4 DIAGRAM SHOWING MOMENTUM AND MAGNETIC MOMENT OF ELECTRONS IN THE DOUBLE-SCATTERING EXPERIMENT OF DE-SHALIT, KURERMAN Et al.

magnetic moment is $\mu = (e\hbar/mc)S$, where μ will be parallel to the electron momentum P, (e is negative). After the scattering at σ_1, P is rotated by 90^o, but the direction of μ is unchanged, so that μ is then at right angles to P (transverse polarization). Finally, with μ pointing upwards, the right-left asymmetry is measured. DE-Shalit et al., show that with the magnetic moment direction as shown in the figure, there will be more particles scattered to the left than to the right. The measured asymmetry for energy 0.9 - 1.7 Mev was $\delta = (5.1 \pm 0.6) \times 10^{-2}$, which is compatible with full polarization. Gursey(27) and Tassee(28) have calculated that for these relativistic energies expected value of δ is $\simeq 9\%$, and the difference between the observed value and the theoretical result is due to plural and multiple scattering in the two foils.

Lipkin et al.,(29) measured the beta ray polarization for Au^{198} by the above method, and found that both for Sn and Au foils, used as σ_2 scatterers, the asymmetry was the same for Au^{198} electrons as for P^{32} electrons, in the same energy range.

ALIKHNOV, ELISEYEV and LUIBIMOV (30) have measured the energy dependence of the polarization of electrons from different sources. The principle of the instrument was the same as that of DE-SHALIT. The spin was changed to transverse by scattering in a thick foil. The twisting

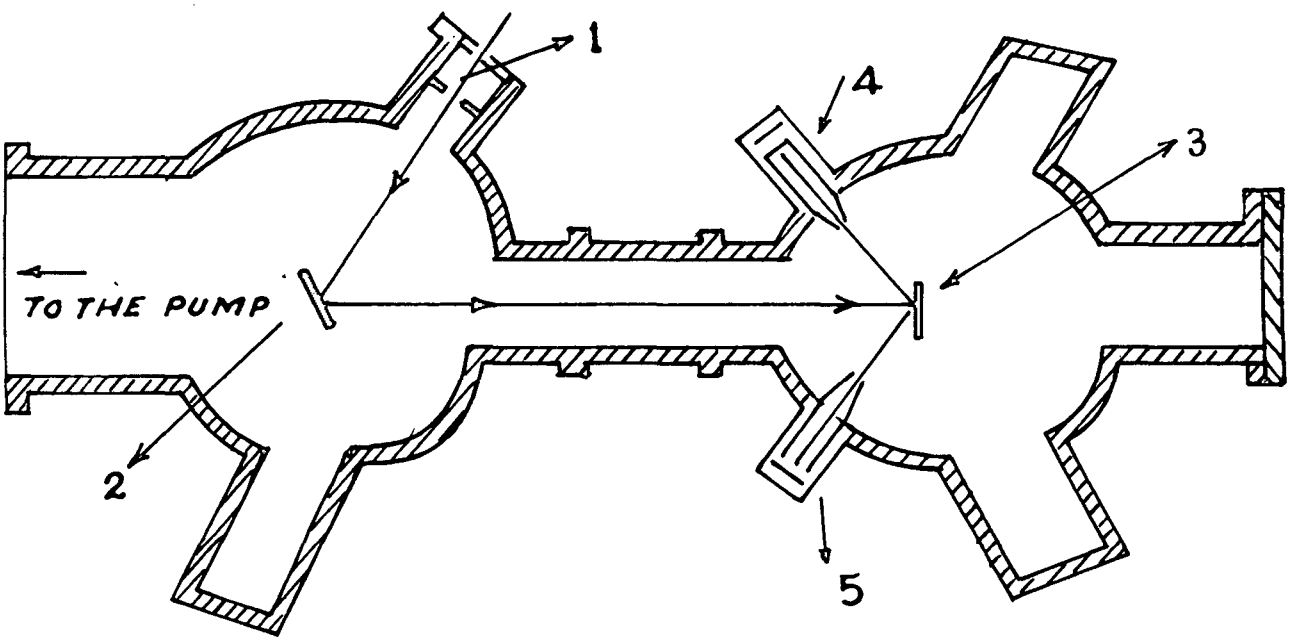

1. ACCELERATED ELECTRON BEAM.
2. FIRST SCATTERER.
3. SECOND SCATTERER.
4, 5. GEIGER COUNTERS.

FIG. 5. APPARATUS OF V.A. APALIN. P.E. SPIVAK. L.A. MIKAELYAN

characteristics of this foil were calculated by Monte-carlo calculation taking multiple scattering into account. Each of the two detectors consisted of a pair of G.M. Counters separated by an energy discriminating absorber and run in coincidence. Corrections were applied for different effects by carrying out many control experiments. The sources used were all first forbidden beta transition with parity shift, viz., Tm^{170}, ($\Delta I = 1$), $R.e^{186}$($\Delta I=1$), Sm^{153} ($\Delta I=1$), Au^{198} ($\Delta I=0$), Lu^{177}($\Delta I=1$ and 0), and for comparison Sr^{90}- y^{90}($\Delta I=2$). For each of these sources, different energy settings were used. The polarization was proportional to v/c within 4 to 7%.

V.A APALIN, P. YE. SPIVAK. L.A MIKAELYAN et al(31) have measured asymmetry with double scattering method, for energies from 45 Kev to 245 Kev and for the angles $\theta_1 = \theta_2 = 120^\circ$, using Au nuclei as second scatterer, and have calculated more accurate values of the function $S(\theta)$ for the above mentioned energy range and for $\theta = 120^\circ$.

The experimental arrangement is shown in fig.(5). After a preliminary magnetic analysis, a well collimated beam of electrons, 12 m.m. in diameter entered a chamber containing the first scatterer. Electrons scattered through 120° passed into a separate chamber with the second scatterer (gold, 16 mg/cm^2), and were detected after scattering through $120^\circ \pm 3$ by two ~~part~~ front surface Geiger counters.

Similar experiments have been done by other workers(32-35).

II-5(ii) Measurements using cylindrical or spherical condensers as a polarization transformer : In a transverse electric field, such as that existing between the plates of a cylindrical or spherical condenser (electrostatic deflector), the electric field is always perpendicular to the momentum. For this case TOLHOEK(36) obtains $\Delta\delta/\Delta\gamma = T_e/E_e$ where, $\Delta\delta$ is the angle by which the spin vector σ is rotated, $\Delta\gamma$ is the angle of deflection of the beam, and T_e and E_e are the kinetic and total energies. The value $T_e/E_e \cong v^2/2c^2$ is negligible, so that $\Delta\delta \cong 0$. Hence, in this case the spin direction remains unchanged, and by deflecting the beam through 90^0, an initial longitudinal polarization can be transformed into a transverse polarization. In order to accomplish the same objective for relativistic electrons, the deflection angle is greater than 90^0 i.e. $=(\pi/2)(1- T_e/E_e)^{-1}$. The deflection voltage that must be applied to the plates of the condensers is given by(37)

$$V_e = \frac{m\gamma v^2}{e} \ln\left(R_2/R_1\right) \quad \cdots \quad (7)$$

for the cylindrical case, and by

$$V_s = \frac{m\gamma v^2}{2e}\left[\frac{R_2}{R_1} - \frac{R_1}{R_2}\right] \quad \cdots \quad (8)$$

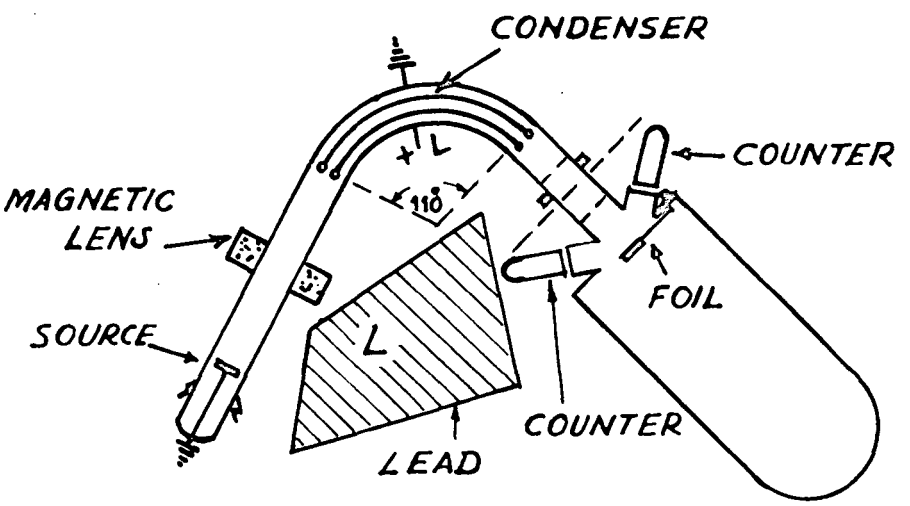

FIG. 6 THE INSTRUMENT USED BY BIENLEIN. WEGENER Et al FOR THE MEASURMENT OF ELECTRON POLARIZATION BY MOTT SCATTERING.

for the spherical case, R_2 and R_1 being the radii of the outer and inner plates.

Frauenfelder et al(38) carried out the first measurement of electron polarization using Co^{60} electrons, using the cylindrical condenser for the transformation of the spin. A deflection angle of 108° was used, and the momentum is turned by 90° with respect to spin. Scattering foils of gold of various thicknesses were used, and the asymmetry was measured for scattering angles from 95° to 140°, by two end window G.M. Counters. A thin source was used to avoid depolarization. The gold foil was then replaced by Al foil to give a measure of the instrumental asymmetry. The polarization was measured for three different groups of Co^{60} electrons, having energies T_e = 50, 86 and 77 Kev. The values of the polarization P obtained from the data are a large fraction (70-80%) of the predicted value $P = -v/c(0.49)$.

BIENLEIN, FLEISCHMANN and WEGNER (39) carried out a rather similar experiment with the instrument shown in fig.(6). The electrostatic condenser is a part of a spherical condenser. The deflection angle is 110° and the scattering angle is about 120°, where the asymmetry is maximum. The magnetic lens is used as an energy selector and also as a focussing device. Better shielding against γ radiation from the source is thus possible. A

large scattering chamber was used, with scattering foils of Al, Ag and Au (50 to 800 $\mu g/cm^2$). The electrons from Co^{60} of energy 166 Kev (v/c = 0.66) gave the value for polarization as (-0.635 ± 0.05).

H-DE-WAARD and J.POPPEMA (40) have measured the longitudinal polarization of beta particles from Co^{60}, P^{32}, Tm^{170} and Au^{198} after deflecting these through 90° in an electrostatic field and scattering from gold foils at angles between 50-87°.

J.S. Greenberg D.P. Malone(41) have measured longitudinal polarization of beta rays from Co^{60} for 194 Kev electrons. The cylindrical condenser was of mean radius 20 cm and a voltage of 25 Kv. was applied to a gap of 1.8 cm. The average scattering angle was limited to 70° in order to get good statistics, plastic scintillators being the detectors. The possible asymmetry due to geometrical factor was investigated. The angular misalignment could lead to a large instrumental asymmetry A and for an angle $\theta' = 1^\circ$ between the beam-axis and the axis of rotation of scattering foil. The value of A could be written as

$$A \simeq \left(X - P S \cos\bar{\phi}_0\right) \sin\bar{\phi}_0 + \left(Y + P \sin\bar{\phi}_0\right) \cos\bar{\phi}$$

The effect of depolarization in the source was also evaluated by using various source thicknesses. This

effect contributed to the maximum uncertainty in the measurements, besides counting statistics.

Thosar et al.,(42) using a hemi-spherical condenser for polarisation transformation have measured the degree of longitudinal polarization for the beta electrons from $Cd^{115\ m}$ ~~was measured~~ at 128 kev, by the method of Mott-scattering for gold and Al scatterer respectively, and a deviation of about 15% was obtained from the statistical rule. It is suggested that the large correction factors found necessary by Sharma and Dvare for the deviation of the shape of the beta transitions, (of higher to the ground~~er~~ state) from straight shape may be due to an accidental cancellation of nuclear matrix element.

A.R. BROSI, A.I. GALONSKY, B.H. KETELLE and H.B. WILLARD (43) have carried out, in detail, the polarization measurement for P^{32} electrons using a spherical electrostatic rotator for the transformation. The electron beam experiences a spin rotation of 62^{o} for 616 Kev electrons. The transversely polarized electron beam was collimated by two 0.5 mm slits before striking the gold target, so as to reduce wall scattering. Four anthracene scintillation counters were fixed at co-planer scattering angles of $\pm$ 30.5^{o} and $\pm$ 135^{o}; the first set of counters measured the instrumental asymmetry. In order to reduce the troublesome effect of backscattering, the forward part of the scattering chamber was made sufficiently large. Gold foils were prepared by vacuum

deposition. The anthracene crystals were cemented to light pipes and connected to Du-mont photomultiplier tubes 6291. Sources of one curie were used to get good counting statistics, obtained by the use of multichannel pulse height analyzer; inspite of this sophistication of instruments, the energy resolution of counters was about 11%. The concurrent measurements of the up-down counting rate was achieved by using two complete detection systems. This made the up and down ratio 'r' independent of source intensity variation and, about half as sensitive as a single detector for background changes, which were measured by rotation of the proper backing material into the scattering position. The experimental results are interpreted in terms of coupling constants. The ratio $C_T/C_A \cong 0.011 \pm 0.010$ is computed.

In all the above mentioned experiments, the usual corrections (see page 20) were applied and results were found to be generally in agreement (within about 10%) with the theoretical expectations.

II-5(iii) Measurements of polarization based on crossed electric and magnetic field arrangement : Crossed electric and magnetic fields can be used to transform the polarization and also select the particle energy. This arrangement is known as Wien-filter. An electron with velocity v travels undeflected through a system of crossed

electric and magnetic fields adjusted so that

$$E \cdot B = 0, \quad B \cdot \hat{t} \times \hat{p} = B \quad \cdots \quad \cdots \quad (9)$$

the particle trajectory is straight if

$$E = -v \times B/c \quad \text{or} \quad |E| / |B| = v/c \quad \cdots \quad (10)$$

It is shown later (see page 45) that

$$\Delta \Phi = e g B L / 2 m c v \gamma^2 \quad \cdots \quad (11)$$

where $\gamma = \left[\left\{ 1 - \left(\frac{v}{c}\right)^2 \right\} \right]^{-\gamma_2}$ and $\Delta \Phi$ is the angle by which the polarization vector has turned after passage through a length L of the Wien-filter.

P.E. Cavanagh, E.F. Turner, C.F. COLEMAN et al(44) were the first to measure the polarization of beta particles from Co^{60} for electrons of energy T_e = 128 Kev $\beta = v/c = 0.6$ using the crossed field arrangement. A thin magnetic lens selects the electrons of a certain energy. The electrons are focussed on to the entrance slit of the B-H field. The electrons are then scattered through 90^0 by a thin gold foil, which is placed in transmission position at 60^0 to the incident beam, in order to reduce the effects of plural scattering in the foil. The two plates providing the electric field were 20 cm long with a gap distance of 2.8 cm. The magnetic field was of the order of 100 oersteds. The detector consisted of a single plastic scintillation counter in connection with a pulse height analyzer, which counts electrons scattered by 90^0 in the gold foil. Several runs were taken for t = 100 $\mu g/cm^2$. Different foils of

thicknesses between 100 $\mu g/cm^2$ to 1 mg/cm^2 were used to estimate plural scattering. The expected $\sin \Phi$ dependence of the asymmetry on the angle Φ between the spin direction and the azimuthal angle of the detector was obtained. Results were obtained with an accuracy of $\pm$ 20% and agreed with the predicted two component neutrino theory. Polarization for 129 Kev electrons from Au^{198} was also measured as $P = (-0.97 \pm 0.20)$ v/c in good agreement with the theoretical results of Benzer-Koller(45). Later on a beautiful modification(46) of the source arrangement was included in the instrument in order to improve the measurement of the energy dependence of the polarization. A potential was applied between the source and the body of the instrument, the electrons are preaccelerated in this potential difference. In order not to change the polarization of the electrons a shield was designed to minimize the transverse electrostatic forces on the electrons In order to measure the energy dependence of the polarization all parameters except the potential were kept constant. The polarization of beta particles was measured in the energy range from 58 to 178 Kev (v/c = 0.45 to 0.70). The curves can be calculated from the relation $P/(v/c) = 1 + \frac{k \delta z}{p}$ adopting different values of k, depending upon coupling constant. They show linear dependence of v/c, although statistics is not good enough.

A.I. ALIKHNOV, G.P. ELISEIV, V.A. LUBIMOV et al(47) have measured the longitudinal polarization P of the electrons from a Sr-y-source corresponding to the transitions $Sr^{90}(0^+) \rightarrow y^{90}(2^-) \rightarrow Z^{90}(0^+)$ and $Sr^{89}(5/2^+) \rightarrow y^{89}(\frac{1}{2})$. A beam of electrons from the source was sent through crossed electric and magnetic fields. The length of the condenser plates was 25 cm, and the gap distance was 12 ± 0.15 m.m. The magnetic field was uniform upto 1.5%. The effective length of the whole system of fields was equal to 27 cm. The electric field was determined to an accuracy of ~ 2%. The magnetic field was measured by a ballistic galvanometer and a standard inductor to within 3%. The source of electrons was in the form of a spot of uniform thickness and diameter 1 cm. on an Al backing. The source thickness was 4 and 1.5 mg/sq.cm. Corrections due to depolarization was calculated from the equation(48) $\cos\theta \simeq 1 - \frac{1}{2}\bar{\theta}^2$, where,

$$\bar{\theta}^2 = 0.157 \frac{z(z^2+1)t}{A(pv/c)^2} \ln\left[1.13 \cdot 10^4 z^{4/3} A^{-1} t\right]$$

The electron beam from the cross field region was incident on the scatterer, fixed at an angle of 45° to the beam axis. Two self quenching G.M. counters were used for counting the electrons in coincidence and were placed at angles of $(90 \pm 4)^\circ$ to the axis of the electron beam. The scattered electrons were always counted in "traversal" to reduce multiple scattering. The instrumental asymmetry

was found by two methods: (a) by replacing the Al foil for gold and (b) by reversing the fields, thus excluding all types of asymmetry except that due to the sign of the field.

The results were accurate to ± 20%, mainly due to low statistics and various associated errors.

P.E. SPIVAK, L.A. MIKAELYAN (49) have measured the polarization of P^{32}, In^{114}, Au^{198}, Lu^{177}, Sm^{157}, Ho^{166}, relatively with respect to Sm^{153}. Absolute values are then calculated at electron energies 300-340 Kev. Beta emitters were situated at a distance of approximately 10 cm above the axis of the apparatus. Electrons that were rotated by a transverse magnetic field through an angle 90^{o} passed through a collimator enclosed in an iron tube, a magnetic guide, and entered the region of the crossed fields. The transversely polarized electron beam again passed through the magnetic guide containing the collimator and fell on the scatterer. The scattered electrons were detected by G.M. counters whose axes were placed at an angle of 120^{o} with respect to the direction of the electron beam. Each of the counters consisted of two counters placed behind each other and connected in coincidence. Between them, there was a filter of thickness 25 mg/cm^2. The device which determined the magnitude of the potential difference across the plates was

calibrated by using known values of the magnetic field and of the energy of conversion electrons passing through the crossed fields. The magnitude of the applied fields corresponded to a rotation of the spin by 90^{o}. The beta source thicknesses varied in the range 0.6-1.3 mg/cm^2. Relative measurements of the polarization were carried out at an energy of 340 Kev. The spectrum of electrons extended approximately from 240 to 440 Kev showing a rather poor resolution. The counter efficiency effect was eliminated by reversing the sign of both the electric and magnetic fields. Values of I_1/I_2 were calculated from the equation,

$$I_1/I_2 = \sqrt{(J_l/J_r)\uparrow \cdot (J_l/J_r)\downarrow}$$

where $J_l\uparrow$ is for field up and $J_r\downarrow$ is for field down of the left and right counts respectively. The background level was kept very low. The relative measurements were carried out under strictly identical conditions. The value of the asymmetry introduced by the apparatus and the spectrum of the electrons falling on the scatterer are not altered with change of sources. The absolute measurements were carried out for Sm^{153} which was the most intense source. The counting rates for the thinnest scatterers amounted to approximately 120, 60 and 30 counts per minute for gold, silver and aluminium respectively. Results of relative measurements show that the polarization of the electrons for the different isotopes are not the same.

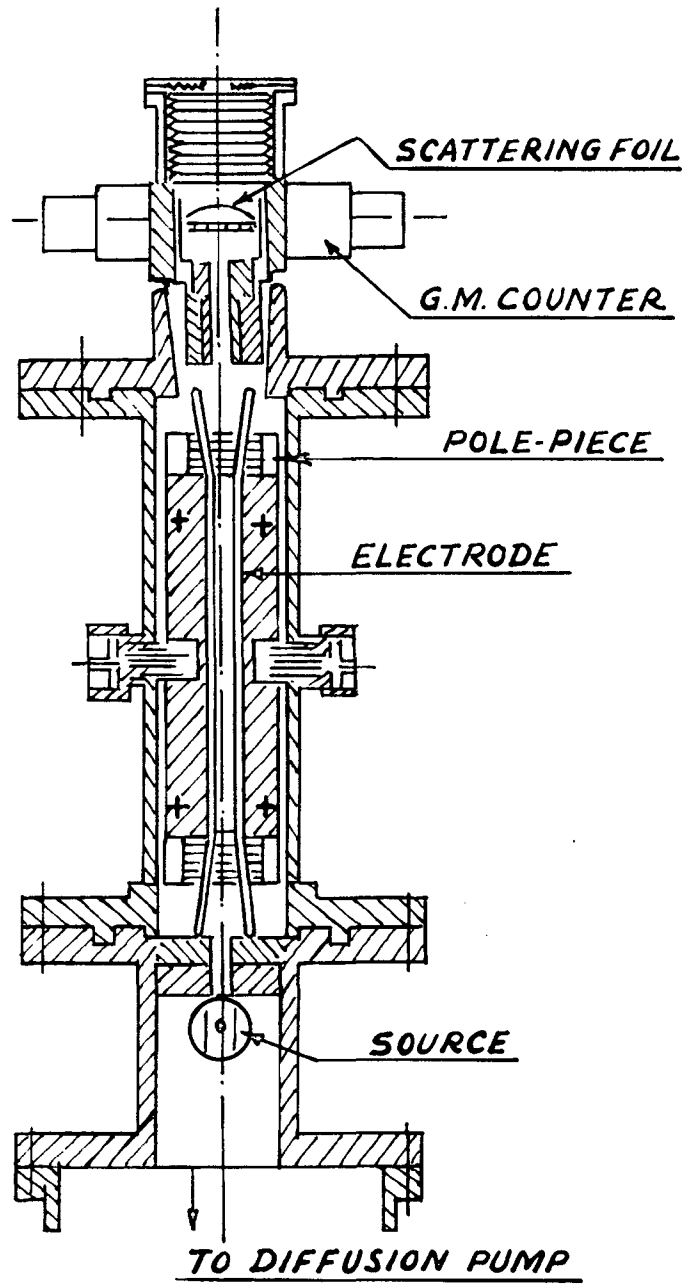

FIG. 7. CROSS SECTION OF THE APPARATUS OF SOSNOWSKIETAL

For example P^{32} and I^{134} for which the transitions are allowed and are of the Gammo-Teller type, polarisation differs by approximately 10%.

R. SOSNOWSKI, Z. WILHELMI and WOITKOWSKA(50) have carried out relative measurements of longitudinal polarization of electrons from beta decay of Na^{24}, Mn^{56}, Sb^{122}, Ho^{166} and Au^{198} for the electrons with v/c=0.85. The choice of the isotopes of highly different atomic numbers was aimed at correlating any departure of the polarization from v/c with the values of Z or A. The cross section of the apparatus is shown in fig.(7). The electron beam striking the scatterer was collimated by two collimators. One of them was placed directly above the source and cut off the electrons scattered by the walls of the apparatus close to the source. The beam collimated by the first aperture was passed through an area limited by electrodes and pole shoes of an electromagnet. For all isotopes, measurements were made for electrons whose velocities were equal to $v/c = 0.85 \pm 0.09$. As a polarization analyzer, a gold foil 1 mg/cm^2 thick was used. It was inclined at 60^0 to the beam axis. The inside walls of the apparatus were covered by lucite to absorb the scattered electrons as well as secondary electrons due to γ-radiation from the source. The electrons scattered at 90^0 were registered by means of G.M. counters

in coincidence. These counters and the gold foil could be rotated about the beam axis. The measurement of the asymmetry consisted in determining the intensity of electron scattering in two directions (a) perpendicular to the plane defined by the beam axis, and (b) in the direction of the transverse polarization.

The number of scattered electrons was obtained from the counting rate with the scatterer in and out. The thickness of the sources used was 1 mg/cm^2 within 15% (size 1 X 2 cm), and the activity varied from 5 to 30 mc. The results of the asymmetry are summarized in table 1.

Table 1

Isotope.	Type of transition.	E_{Mean} kev.	Asymmetry %
Na^{24}	$4^+ \longrightarrow 4^+$	1400	11.0 ± 0.9
Mn^{56}_{25}	$3^+ \longrightarrow 2^+$	1890	11.1 ± 0.8
	$3^+ \longrightarrow 2^+$		
	$3^+ \longrightarrow 2^+$		
Sb^{122}_{51}	$2^- \longrightarrow 0^+$	1570	10.1 ± 0.3
	$2^- \longrightarrow 2^+$		
Ho^{166}_{67}	$0^- \longrightarrow 2^+$	1800	10.4 ± 0.2
	$0^- \longrightarrow 0$		
Au^{198}_{79}	$2^- \longrightarrow 0^+$	966	9.3 ± 0.3

Although identical conditions of measurement were aimed at,

there are several factors which may have influenced the results and consequently may have been different for various isotopes. The following are the most important ones:

(a) The shape of the beta spectrum(maximum energy)

(b) Gamma spectrum associated with beta.

(c) The material of the source.

(d) The activity of the source.

The effect of the first factor cannot be very important, since, for all isotopes under investigation, the point representing $v/c = 0.85$ was on the resting part of the curve, making the spectrum of electrons similar for all isotopes inspite of low resolution. The effect from gamma radiation was taken into account by measuring the background from each source. It was found that the introduction of the gold foil did not change the number of secondary electrons reaching the counter. The depolarization in the source was identical and also small for the thicknesses of the sources used. As mentioned above, the activities of the sources were different, and the results would have been connected with the error due to the dead-time of the counters. The weaker sources, however, had a much higher gamma background and the counting rates were not very much different from source to source. Dead-time corrections had to be introduced only for Au^{198}. These authors were not sure of any systematic errors in their

measurements, yet, they generally indicate that the electron polarization is not constant for all the isotopes. For the hypothesis that the polarization is constant, the X^2-parameter takes on a value 12.37, for $\mathcal{L} = 0.02$. This hypothesis should be discarded. In assuming a linear decrease in polarization with Z for $P = 1 - 0.002 \times Z$ determined by the least square method, $X^2 = 5.85$ was obtained. Therefore, this hypothesis is much more probable and cannot be discarded even for $\mathcal{L} = 0.05$.

It may be noted from the above review of the previous work in this field that, the picture is not quite clear regarding the exact dependence of polarization on factors such as the atomic number Z of the emitting nucleus, the energy and polarization of the incident electrons, and the nuclear structure. As a result deviations from full polarization (v/c) have been observed in many experiments.

It was thought, therefore, interesting to study these aspect with an improved experimental system, in which the errors could be more definitely calculated and the results could then throw more light on this factor.

Chapter III discusses the experimental set up designed and fabricated by the author.

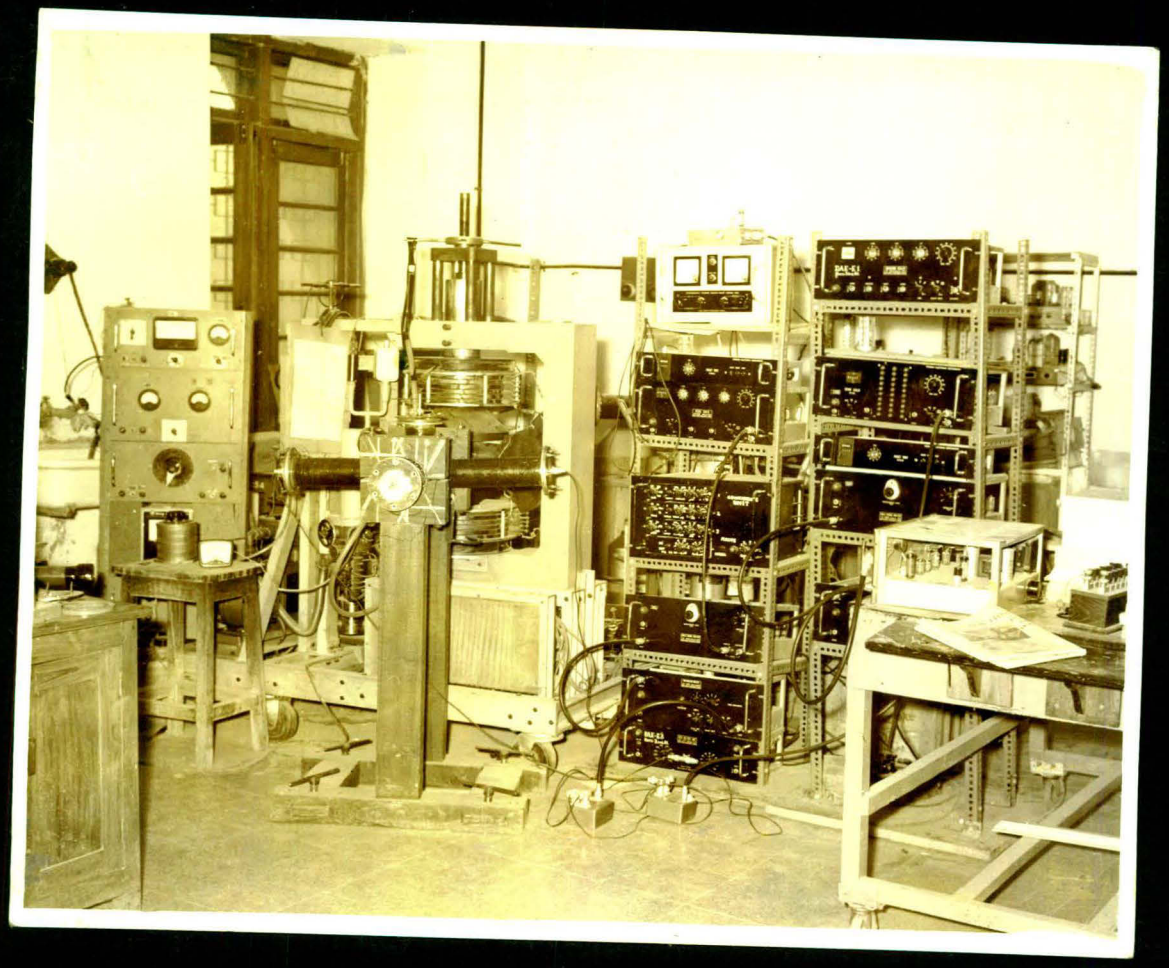

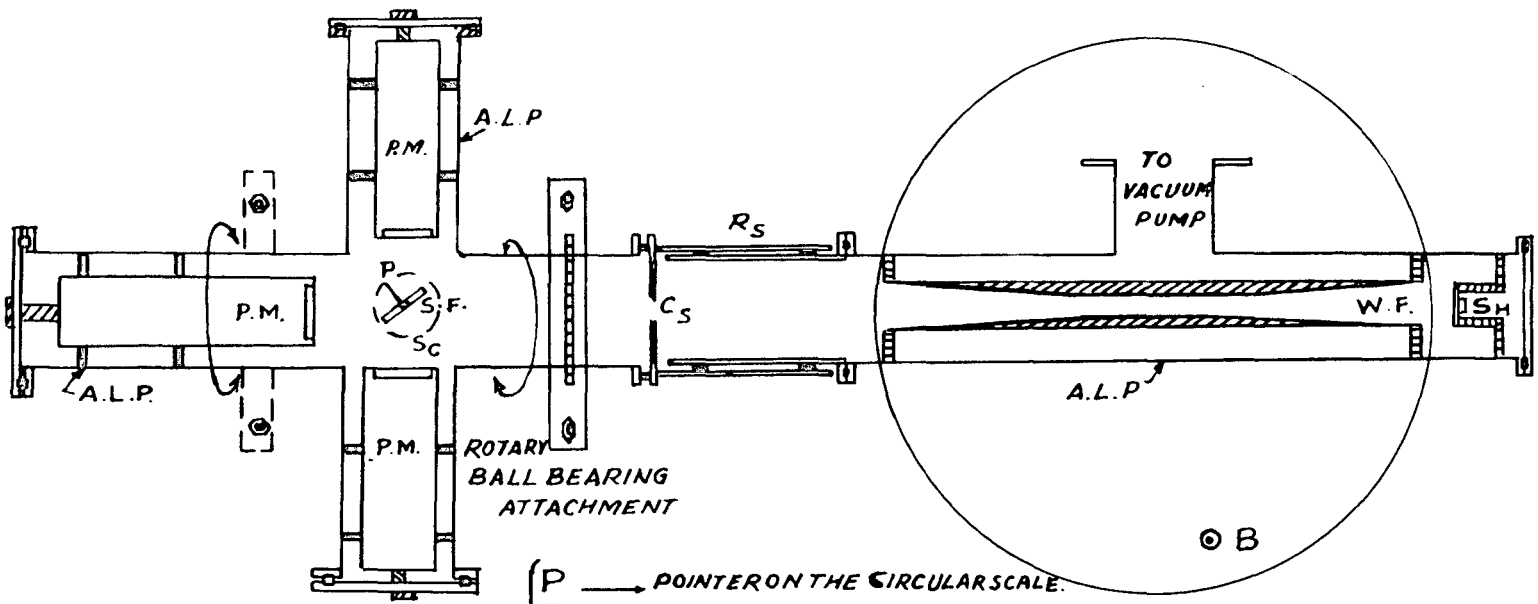

P ⟶ POINTER ON THE CIRCULAR SCALE.
S_H ⟶ SOURCE HOLDER
⊙B ⟶ EFFECTIVE MAGNATIC FIELD SPACE.
W.F. ⟶ WIEN FILTER, IN WHICH GRADIENT OF 20% ON 6 Cm LENTH ON EITER SIDE IS MADE TO ANNUL MAGNETIC FRINGING.
R_S ⟶ ROTATING SEAL ARRANGEMENT TO PLACE THE SCATTERING CHAMBER IN ANY AZIMUTH ABOUT THE BEAM AXIS
C_S ⟶ COLLIMATING SLIT.
S.F. ⟶ SCATTERING FOIL OF GOLD ETC.
Sc. ⟶ CIRCULAR SCALE — $\pm$ 0.5° FOR MEASURING ROTATION OF THE SCATTERING FOIL.
P.M. ⟶ PHOTOMBLTIPLIER-WITH SUITABLE SCINTILLATOR.
A.L.P. ⟶ ALKATHENE PIPE FOR HOUSING-SCATTERING CHAMBER; CONDESER PLATES, ETC.

FIG. 8. SCHEMATIC DIAGRAM OF THE EXPERIMENTAL SET UP

CHAPTER III

THE EXPERIMENTAL SET UP

III-1. General Description:

The experimental set up consists mainly of two parts: (i) A Wien-filter, and (ii) Scattering chamber. A systematic diagram of the whole system is shown in fig.(8) and described briefly below:

(i) The Wien-filter part (W.F.) consists of :

(a) The condenser plates, fixed in a perspex frame.

(b) The beta ray magnet with large circular pole-pieces (⌀ B).

(c) The beta ray source holder (SH) also containing the first collimating aperture for the emergent beam.

(d) The vacuum system coupled to the Wien-filter which evacuates the system upto 10^{-4} mm.Hg.

(e) The high voltage unit (see fig.(13)) which supplies voltages upto 32 kv.

(ii) The scattering chamber part consists of :

(a) A rotating seal arrangement (RS) which enables the scattering chamber to be rotated freely and placed in any azimuthal plane from 0^{o} to 360^{o}.

(b) A second collimating slit C_s.

(c) A scattering foil holder (S.F.) which enables

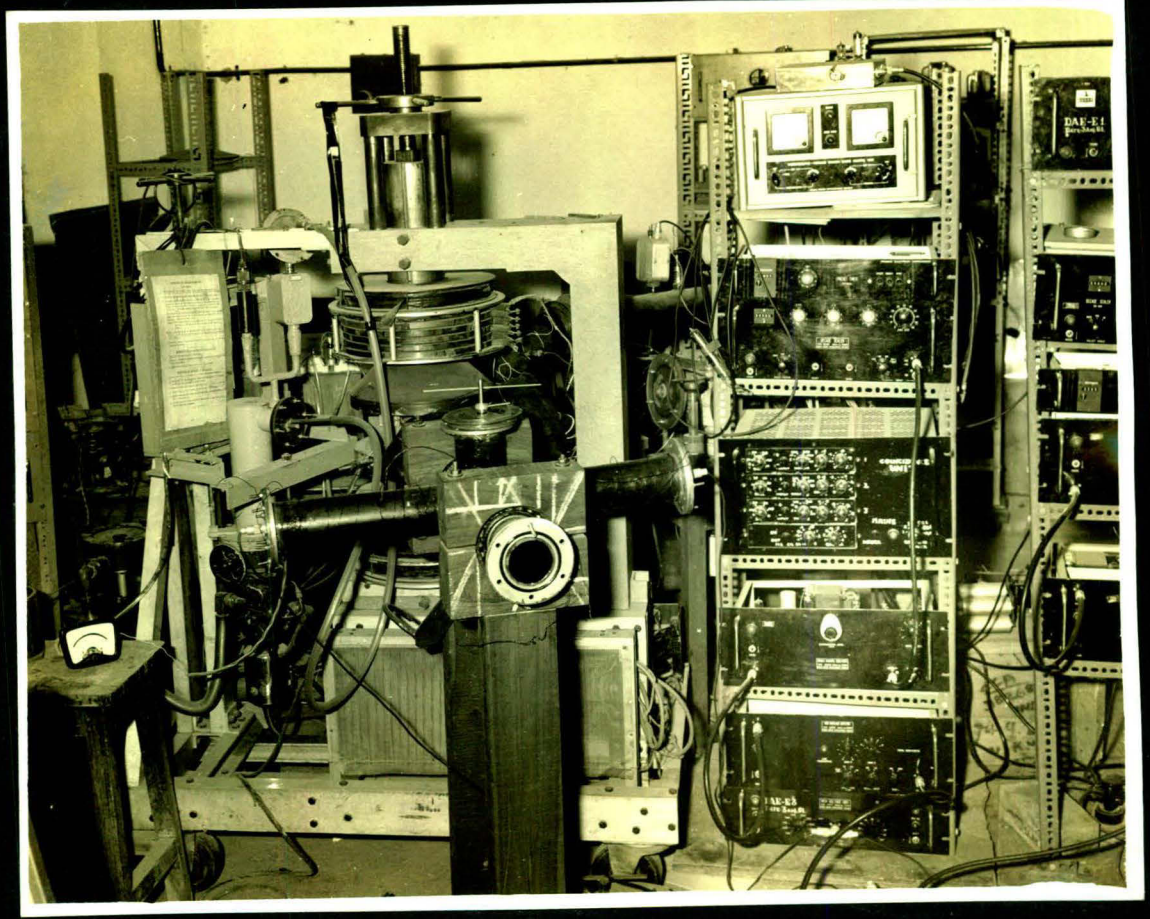

easy manipulation to be done from outside the vacuum system. The foil by this arrangement could be inserted or taken off the beam direction, or rotated about the beam axis.

(d) Two identical plastic scintillation counters (P.M.) placed symmetrically about the beam axis, to detect simultaneously electrons scattered at 90^{o} for measurement of the L-R asymmetry.

(e) A third scintillation counter (P.M.) is placed directly in front of the incident beam for measuring the beam intensity.

(f) Two separate electronic channels for counting the output pulses from the scintillation counters consisting of a pre-amplifier, a non-overload amplifier and a pulse height analyzer with a scaler coupled to an electronic timer.

The salient features of the design and construction of the main parts of this equipment are now described in the following sections of this chapter.

III-2 Polarization Transformer:

Out of the three methods described earlier (p.21) for transforming the longitudinal polarization into transverse one, for the Mott scattering method of analysis used in these experiments, we have selected the Wien-filter method (p. 28). This was considered to be the most

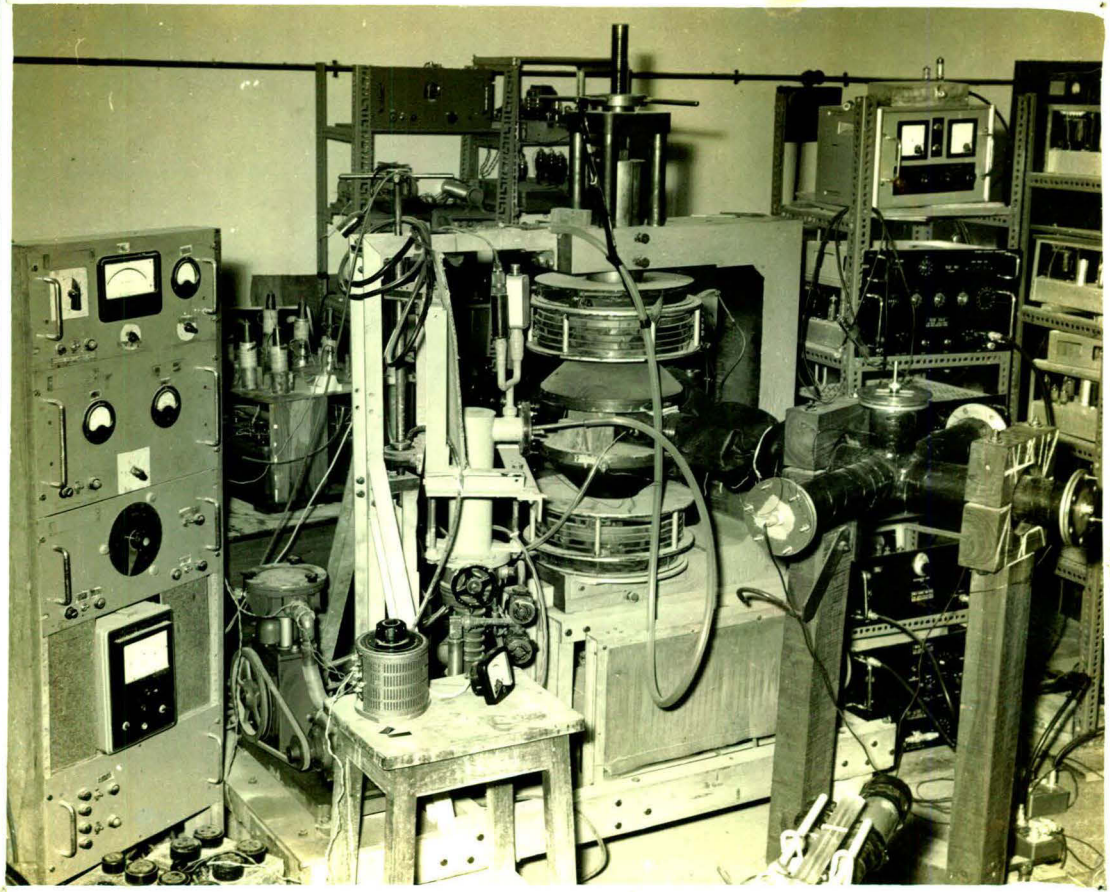

suitable for the present work, as it possesses the following advantages over the other polarization transformation methods.

(a) The entire arrangement is axially symmetric thus reducing appreciably the magnitude of the experimental asymmetry effects.

(b) The magnetic (B) and electric (E) fields can be varied in such a way that the degree of transformation of the polarization ($\Delta\Phi$) can be varied continuously up to the full value (90^{o}) for a wide range of energies.

(c) Since the maximum change in polarization can be chosen to be the full value (90^{o}), errors $[d(\Delta\Phi)]$ in spin rotation due to an error (dL) in determination of the effective length L, are small, thus causing inappreciable errors in v/c.

(d) By reversing B and E simultaneously, the geometry of the apparatus remains unchanged, but $\Delta\Phi$ changes sign. This property allows a simple elimination of asymmetry effects, due to different counter, efficiencies and other instrumental asymmetries such as those mentioned in (c).

(e) This device can be used as a velocity selector and simultaneously as a polarization transformer.

III-3 Theory of the Wien-filter :

III-3(i) Introduction :-

In order to study the variation of the polarization in external electromagnetic fields, we define the angle Φ between the polarization vector P and the momentum unit vector $\hat{p}$ as

$$(P.\hat{p})/P \equiv \cos \Phi \quad \text{- - - - - - - - - - - - - - - (12)}$$

In an external electromagnetic field, Φ will, in general, be a function of time. The laboratory time rate of change, $d\Phi/dt$, in a homogeneous field is given by(51,52)

$$\Omega = \frac{d\Phi}{dt} = \frac{e}{2mc}\left\{\frac{\hat{t}.E}{(v/c)}\left[(g-2) - \frac{g}{\gamma^2}\right] + \hat{t}.(p\times B)(g-2)\right\} \cdots (13)$$

In this equation E and B denote the electric and magnetic field strengths; $\hat{p}$ and $\hat{t}$ are unit vectors in direction of the momentum and the transverse polarization respectively, v is the particle velocity; the rest mass and charge are m and e; while, the dimensionless g factor is defined as the ratio of the magnetic moment μ to the spin S ; and $\gamma = \left[1 - (v/c)^2\right]^{-\frac{1}{2}}$. For negative Dirac particles, i.e., electrons, the magnetic moment points opposite to the spin. Equation (13) is valid as long as the distances over which the fields vary are large compared to the dimensions of the wave packets describing the particle. Inhomogeneous fields are also discussed by Good et al.,(53).

The magnetic and electric fields could have

different relative dispositions and these cases are discussed briefly below.

III-3(ii) Longitudinal fields:

Assuming the electric and the magnetic fields as parallel to the momentum:

$$E \times \hat{p} = 0 \qquad B \times \hat{p} = 0,$$

the longitudinal polarization remains constant. The transverse polarization is affected in two ways. In a longitudinal magnetic field, the maximum transverse polarization also remains constant (Φ = constant), but the transverse polarization precesses around the field direction with an angular frequency:

$$\omega_B = g\ e\ B/2\ mc\gamma = g\mu_0 B/\hbar\gamma \quad \text{- - - - - - - - - (14)}$$

This rotation can be used for direct determination of the g factor of the free electrons. In a longitudinal electric field, the transverse polarization remains unchanged in the rest system of the particle. The electric field, however, changes the total energy W of the particle. According to equation $P_t\ (Lab) = \frac{mc^2}{W} P_t\ (rest)$, the transverse polarization observed in the laboratory system will then change suitably.

III-3(iii) Transverse electric field:

Assuming an electric field which is always

perpendicular to the momentum:

$$B = 0,\ E.\hat{t} = E,\ E.\hat{p} = 0,$$

the trajectory in such a field will be circular and the laboratory angular frequency of the particle will be given by

$$\omega_E = eE/m\gamma v \qquad \ldots \qquad \ldots \qquad (15)$$

The momentum will also rotate with a frequency ω_E. The polarization angle Φ changes according to

$$\frac{d\Phi}{dt} = -\Omega_E = \tfrac{1}{2}\omega_E\left[(g-2)\gamma - g/\gamma\right] \qquad \ldots \qquad (16)$$

If Φ_o is the polarization angle of a particle before entering the electric field, and if the momentum is turned by an angle $\Delta\psi$ by the electric field, the polarization angle becomes $\Phi' = \Phi_o + \Delta\Phi$, where, $\Delta\Phi = \tfrac{1}{2}\Delta\psi\left[(g-2)\gamma - g/\gamma\right]$ and the angle $\Delta\psi$ required to transform longitudinal into transverse polarization completely ($\Delta\phi = -\pi/2$) is given by

$$\Delta\psi = \frac{\pi\gamma}{g-(g-2)\gamma^2} \qquad \ldots \qquad \ldots \qquad (17)$$

In the non-relativistic limit, since $\gamma = 1$, the situation becomes more simple. It follows that $-\Omega_E = -\omega_E$. As seen in the laboratory system, the polarization vector keeps its direction in space and thus, the polarization direction is not affected by the electric field. The angle $\Delta\psi$ becomes $\pi/2 (g=2)$ for electron.

III-3(iv) Transverse magnetic field:

In a transverse magnetic field $E = 0$, $B.\hat{t}\times\hat{p} = B$,

the time rate of change of the polarization angle becomes

$$\Omega_B = \frac{eB}{2mc}(g-2) \quad \ldots \quad \ldots \quad (18)$$

The orbital angular frequency of a charged particle in this field is given by the Larmor frequency

$$\omega_L = \frac{eB}{m\gamma c} \quad \ldots \quad \ldots \quad (19)$$

Hence, $\Omega_B = \frac{1}{2}\omega_L\gamma(g-2)$ ... ... (20)

and that for the special case of an electron with $g = 2$, there will be precession in a transverse magnetic field without change of the polarization angle Φ. A particle with $g \neq 2$, such as mesons, on the other hand, will suffer a change of the polarization angle and this change is used to determine the anomalous part $a = \frac{1}{2}(g-2)$ directly for free electrons and free muons.

III-3(v) Crossed fields:

Consider transverse crossed fields,

$$E.B = 0, \quad B.\hat{t} \times \hat{p} = B \quad \ldots \quad \ldots \quad (21)$$

adjusted in such a way that the particle trajectory is straight giving

$$E = -v \times B/c \quad \text{or} \quad E/B \equiv |E| / |B| = v/c \quad \ldots \quad (22)$$

The laboratory time rate of change of Φ, $\frac{d\Phi}{dt}$ in a homogenous field is given by

$$\Omega_{EB} = \frac{d\Phi}{dt} = \frac{e}{2mc}\left\{\frac{\hat{t}.E}{(v/c)} - \frac{g}{\gamma^2}\right\} + \hat{t}.(\hat{p} \times B)(g-2) \quad \ldots \quad (23)$$

Inserting equation (21) and equation (22) in equation (23)

and as the second term vanishes for g=2 particles(electron) we get

$$\Omega_{EB} = \frac{d\vec{\Phi}}{dt} = \frac{e}{2mc}\left\{\frac{\hat{t}.E}{(v/c)}\left[-\frac{g}{\gamma^2}\right]\right. \quad \ldots \quad (24)$$

and by putting $E = -v \times B/C$ we get

$$\Omega_{EB} = \frac{d\vec{\Phi}}{dt} = \frac{e}{2mc}\left\{\frac{\hat{t}.(-v \times B/C)}{v/c}\right\}\left[-\frac{g}{\gamma^2}\right] \quad \ldots \quad (35)$$

hence

$$\Omega_{EB} = \frac{d\vec{\Phi}}{dt} = \frac{e}{2mc}\left\{\frac{\hat{t}.(\times B)g}{\gamma^2}\right\} = \frac{egB}{2mc\gamma^2} \quad \ldots \quad (26)$$

and the polarization vector is turned by an angle

$$\Delta\Phi = \frac{d\vec{\Phi}}{dt} \times dt = \frac{d\vec{\Phi}}{dt} \cdot \frac{L}{v} \quad \ldots \quad (27)$$

where, L is the length of the crossed field and v is the velocity of the electrons, substituting eq.(26) in eq.(27) we get

$$\Delta\Phi = \left\{\frac{egB}{2mc\gamma^2} \cdot \frac{L}{v}\right\} = \frac{egBL}{2mc\nu\gamma^2} \quad \ldots \quad (28)$$

For a complete transformation from longitudinal to transverse polarization

$$\Delta\Phi = \pi/2 = \frac{egBL}{2mc\nu\gamma^2} \quad \ldots \quad \ldots \quad (29)$$

the required value of the magnetic field is

$$B = \frac{\pi mcv\gamma^2}{egL} \quad \ldots \quad \ldots \quad (30)$$

III-4(i) Design calculations:

From equation (28) of section III-3, the calculations

of the design parameters are carried out as follows:

$$\Delta\Phi = egBL/2mc\, v\, \gamma^2$$

putting $v/c = \beta$

$$\Delta\Phi = egBL/2mc^2\beta \quad \ldots \quad \ldots \quad (31)$$

since $\gamma^2 = \frac{1}{1-\beta^2}$

$$\Delta\Phi = \frac{egBL\,(1-\beta^2)}{2mc^2\,\beta} \quad \ldots \quad \ldots \quad (32)$$

also for electron $g = 2$, $\frac{e}{m} = 5.28 \times 10^{17}$ e.s.u. $c^2 = 9 \times 10^{20}$

hence $\Delta\Phi = \frac{0.586}{10^3} L \frac{(1-\beta^2)}{\beta} B \quad \ldots \quad (33)$

In the present system L = 32 cm (see p. 48)

$$\therefore \Delta\Phi = \left[\frac{18.75}{10^3}\right] B \frac{(1-\beta^2)}{\beta} \quad \ldots \quad (34)$$

The values of B (mag. field) for various beta values (v/c) and for different degrees of transformation of polarization (for various $\Delta\Phi$) are shown in table (2). The values of electric field E are calculated by equation $E = \beta \times B \times 300$ volts./cm

Table 2

$\Delta\Phi$	β =(v/c)	Corresponding K.E. of electrons (kev)	B in Gauss.	E in kV/cm.
$\frac{\pi}{2} = 90^\circ$	0.5	79	56	8.4
Full transformation	0.6	127	78	14.0
	0.7	204	115	24.1
	0.8	340	186	44.6
	0.9	661	398	107.46
$\Delta\Phi = \frac{\pi}{3} = 60^\circ$	0.5	79	37	5.5
	0.6	127	52	9.36
	0.7	204	76	16.0
	0.8	340	124	29.8
	0.9	661	266	72.0
$\Delta\Phi = \frac{\pi}{4} = 45^\circ$	0.5	79	28	4.2
	0.6	127	39	7.0
	0.7	204	57.5	12.0

III-4(ii) Selection of various design parameters:

(a) Scattering angle θ :- It was decided to choose 90° as the scattering angle for the present work; because it is geometrically convenient for the apparatus symmetry, and secondly, although the asymmetry (a) is maximum at

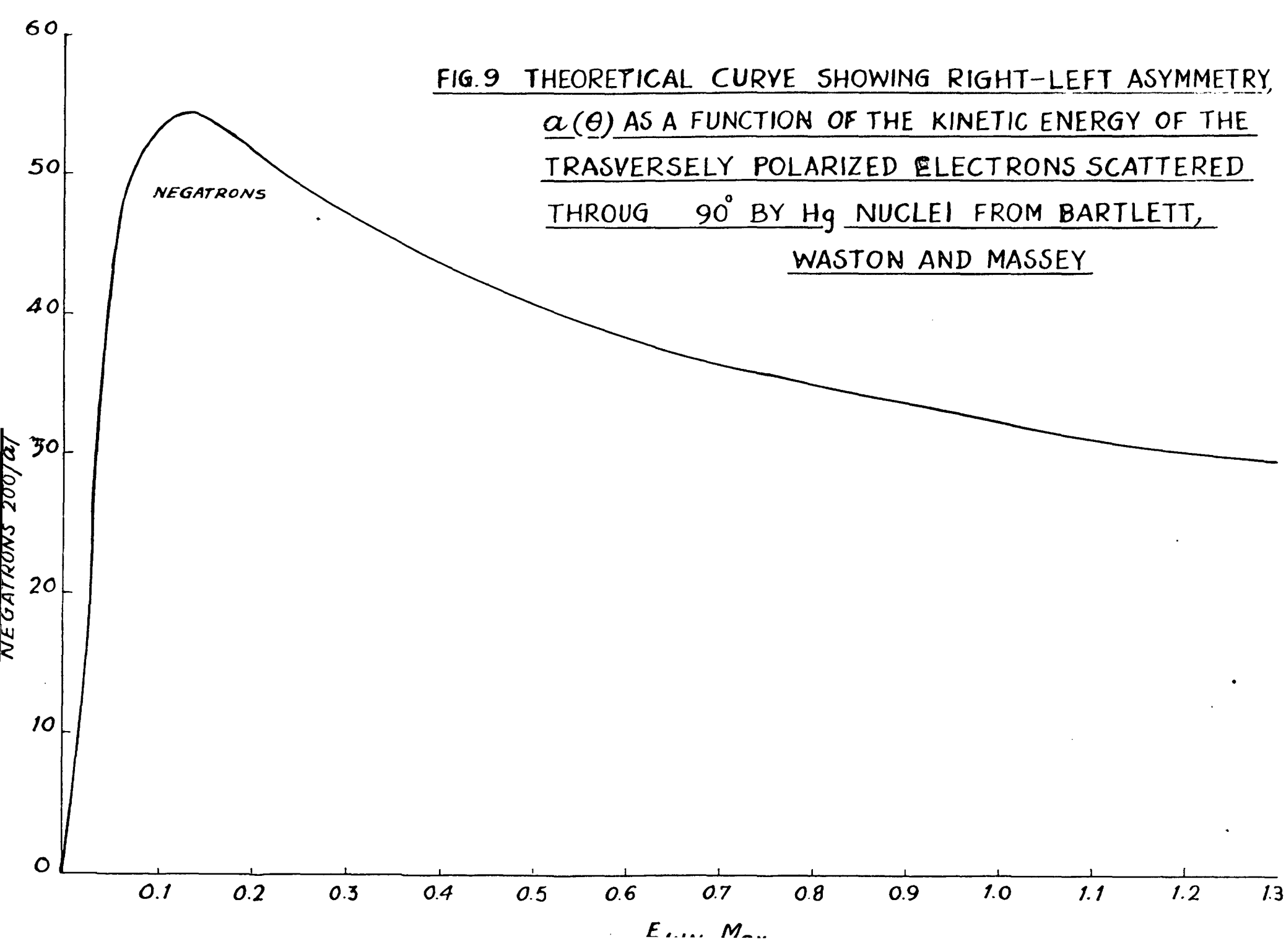

FIG. 9 THEORETICAL CURVE SHOWING RIGHT-LEFT ASYMMETRY, $a(\theta)$ AS A FUNCTION OF THE KINETIC ENERGY OF THE TRASVERSELY POLARIZED ELECTRONS SCATTERED THROUG 90° BY Hg NUCLEI FROM BARTLETT, WASTON AND MASSEY

120^{o}, the intensity of the beam is better at 90^{o} then that at 120^{o}. It is known that Mott scattering cross-section falls off rapidly with scattering angle. Thus, for $\theta = 120^{o}$; $a(120^{o}) = -0.424$, and $\frac{d\sigma}{d\Omega}$ (2.0×10^{3} barns/sterad) is down by a factor of 2 from its value at 90^{o}(4.29×10^{3} barns/sterad). It was not possible to use sources of high activity in our experiment. The only way, therefore, to achieve good statistics without sacrificing the intensity of the beam was to fix the counters at 90^{o}.

(b) Beta value (v/c) or energy of electrons:- The value of beta was taken as $v/c \simeq 0.6$, as the asymmetry function $|a(\theta)|$ for 90^{o} and $Z = 79$ (Au) is highest(54) for $v/c = 0.6$ as will be seen from the variation shown in fig.(9).

(c) The length of the crossed field L was adjusted to be equal to 32 cm. This was determined by the size of the pole-pieces of the beta-ray magnet, in such a manner as to utilize the maximum available extent of the magnetic field. However, as mentioned in para (f), a small fringing field effect probably remains even after the use of screening pipes. This causes an error less than $\pm$ 0.2cm in the effective value of L.

(d) Electric and Magnetic fields: The values of these fields ($B \simeq 78$ gauss, $E \simeq 14$ kv/cm) for $\beta = 0.6$ and $\Delta\Phi = \pi/2$ were taken from table 2.

FIG. 10. MAGNETIC FIELD GRADIENT ALONG THE CENTRAL AXIS IN THE HORI. PLANE

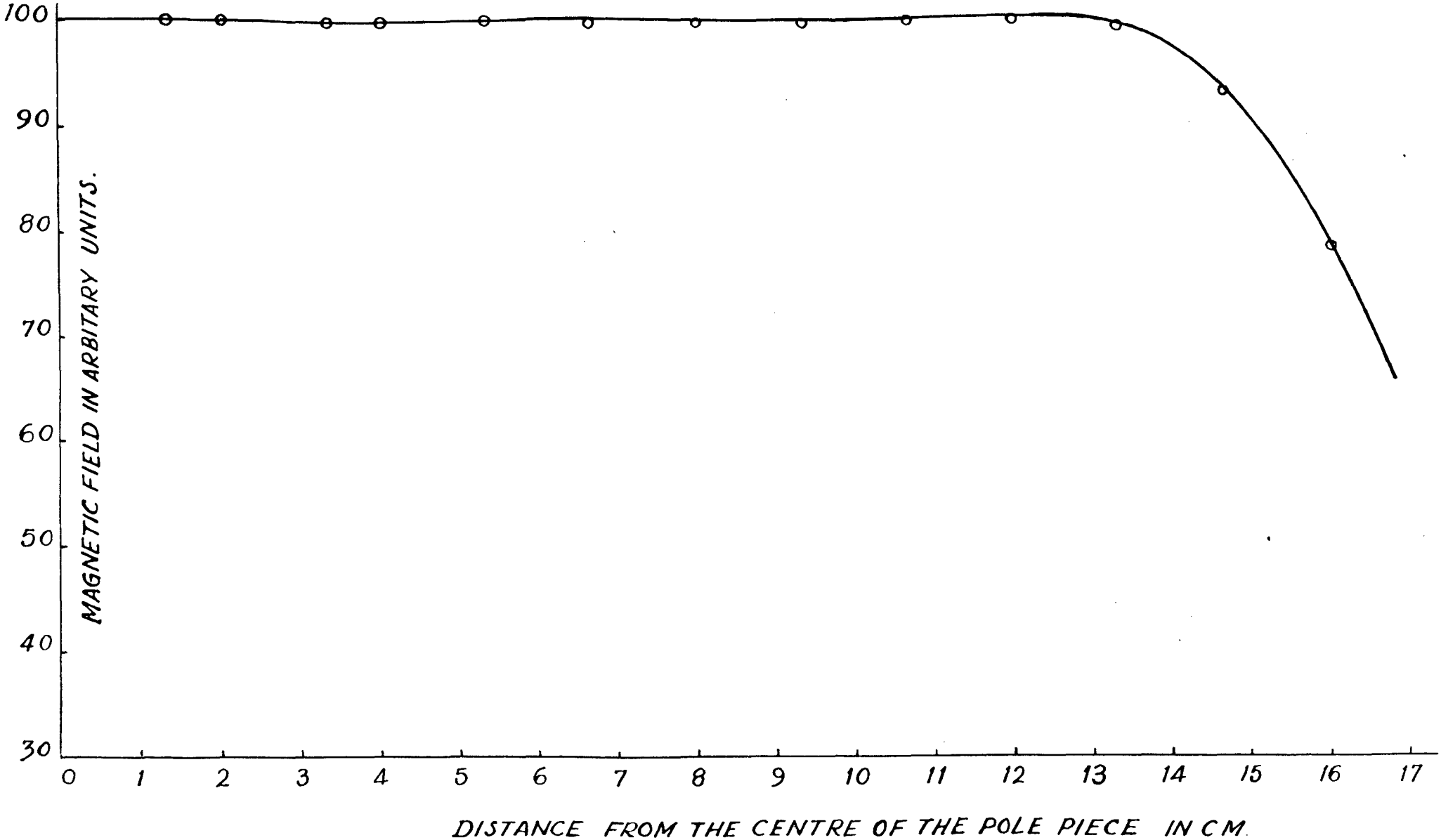

(e) The gap length between the plates: The required strength of the electric field could be obtained in various gap lengths upto a maximum of 2 cm for the voltage source of about 32 kV, that was constructed in this laboratory. However, the other important factor fixing the size of the gap length as 1 cm was the occasional Corona discharges, occurring on the condenser plates, inspite of the extreme care taken in giving the plates a high polish and smoothness. This also ensures a high stability of the voltage which was now fixed at 14 kV about half the maximum rating.

(f) The tapering in condenser plates for uniform field ratio (E/H): The gradient of the magnetic field was found out by a Hall probe gaussmeter, which was moved over a graduated scale along the central axis of the magnetic field in the horizontal plane, and the variation from the centre of the magnetic field to a sufficiently large distance beyond the extent of the pole-pieces, was studied. This variation is shown in table 3 and plotted in fig.(10).

The condenser plates of aluminium were tapered at the ends as shown in fig.(14) so as to provide equal gradients in the electric field and the magnetic field. Hence, the ratio (E/H) of the two fields remains the same, all along the crossed field region.

Table 3

Distance from the centre of the field in cm.	Field in arbitrary units.	Distance from the centre of the field in cm.	Field in arbitrary units.
0	100	12	100
1	100	13	100
2	100	14	95
3	100	15	90
4	100	16	80
5	100		
6	100		
7	100		
8	100		
9	100		
10	105		
11	105		

III-5(i) Magnetic Field:

The beta ray spectrometer magnet was used in the present experiment. The magnet can provide a uniform field upto 1300 gauss, at the maximum current of 15 amps in the main coil. The gap between the pole pieces is adjustable and has a maximum separation of 6 inches. The cross section of the yoke, pole blocks, and pole pieces are shown fig (11

The pole blocks are detachable and are of nearly 13 inches (32.5 cm) in

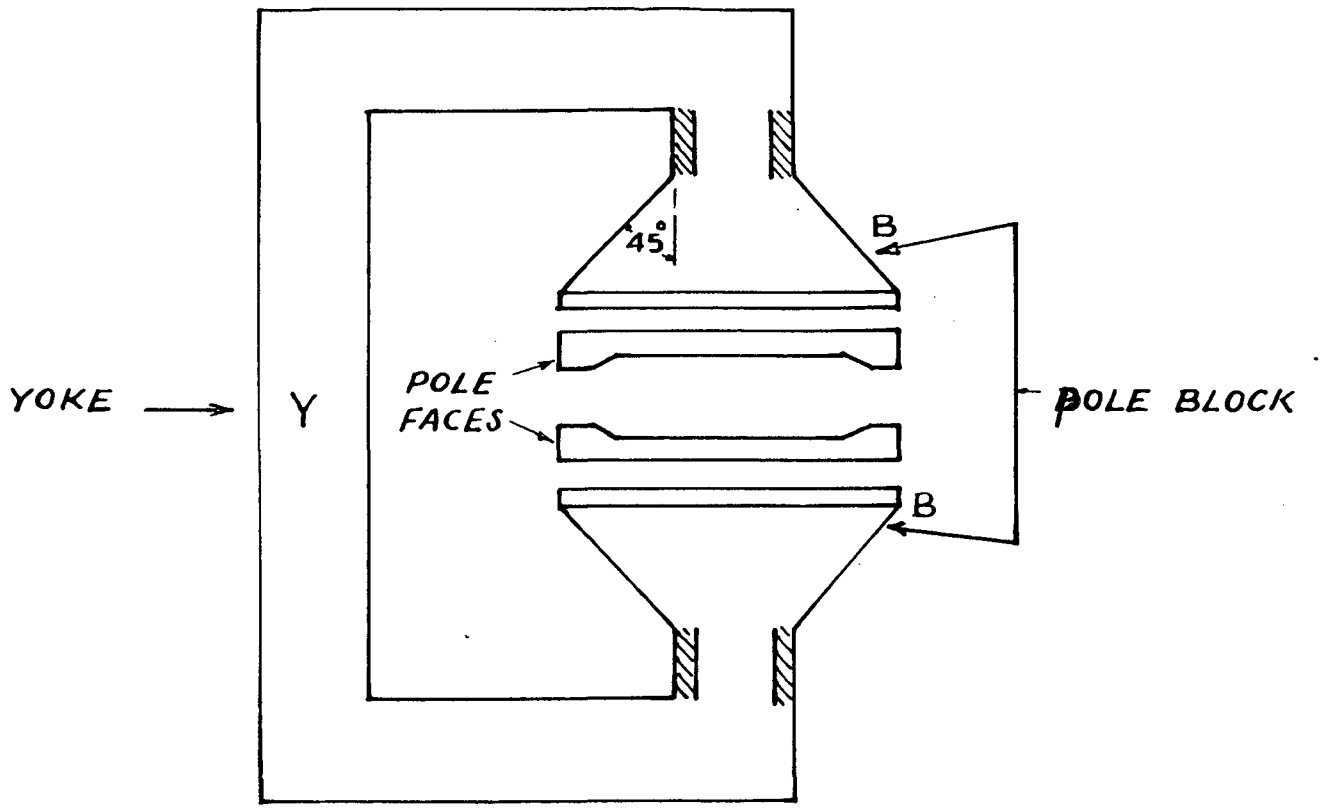

FIG. 11. THE CROSS SECTION OF THE YOKE POLE BLOCKS & THE POLE FACES

diameter at the bottom and of about 6 inches at the top. The tapering on these blocks is of 45^{o}. To prevent excessive distortion of the field in the gap by the leakage of flux to the yoke (Y) of the magnet, the smallest distance from the edge of the pole faces to the nearest part of the core was $6\frac{1}{4}$ inches.

The pole faces were shimmed in such a way that the edges were raised, thus, the field tended to remain constant even near the edges. This increased the area of the uniform field region between the poles. The main coil was split into two parts and each was placed on either side of the air gap. This arrangement reduced the leakage flux. The inner diameter of the coil was 5 inches and the outer diameter was about 13 inches. The coil consisted of copper strips of $\frac{1}{2}$" x 0.025" and can carry a current of 15 amps. Each half of the coil had 685 turns and was wound in six pancake type layers separated from each other and from the steel tube over which these were wound. The gaps left between the layers and the steel tube enabled the windings to be cooled by forced air, if necessary.

The D.C. resistance of the coil at room temperature was about 2.5 ohms. To protect the coil from surges, which usually appear when the current is broken suddenly, Metrosil, non-linear resistances, were connected directly across each half of the coil. The change over relay in

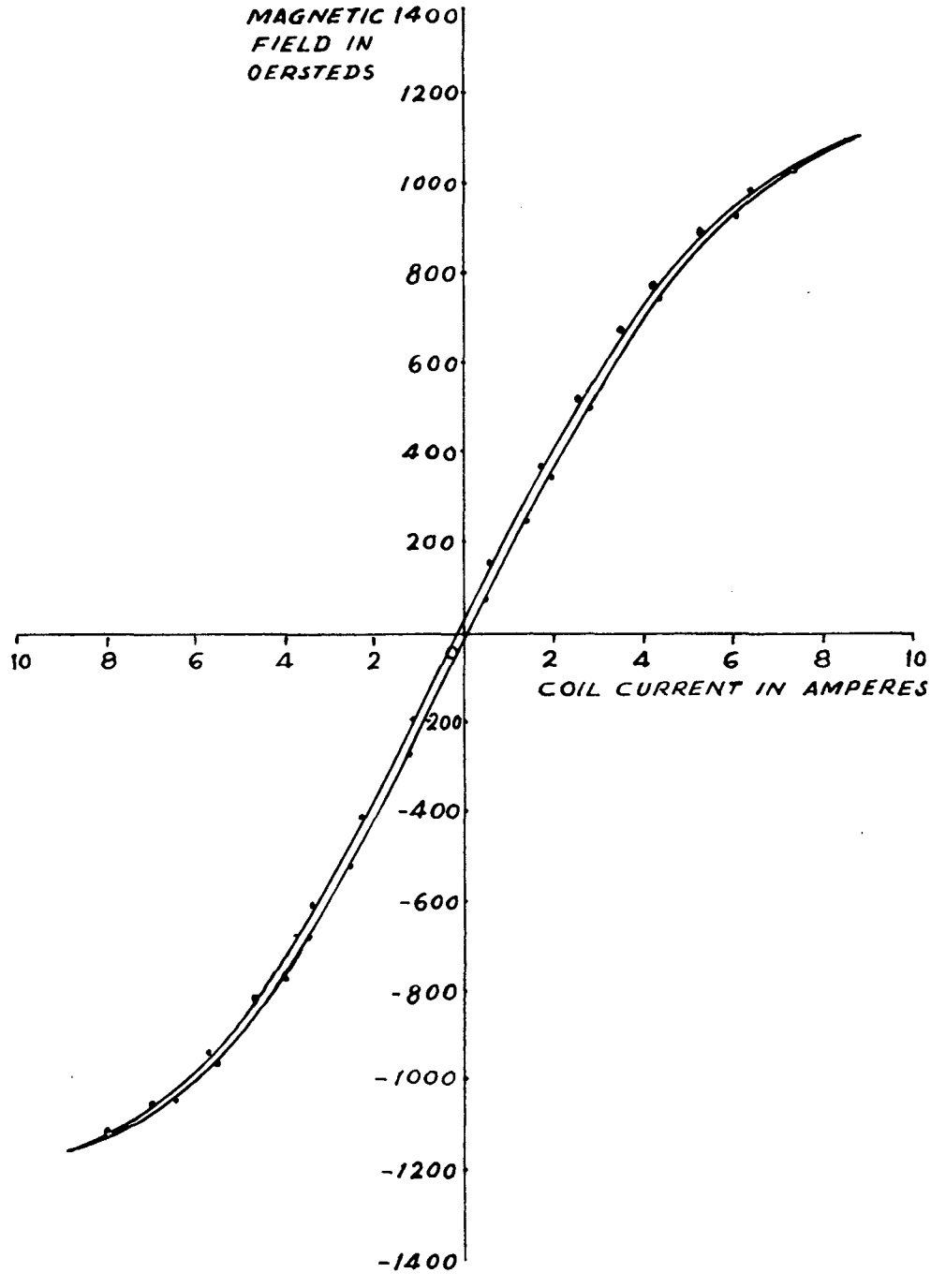

FIG. 12 HYSTERESIS LOOP OF THE MAGNET

the main coil circuit can reverse the direction of the current. An inter-locking relay is provided, which prevents the reversing relay being operated when the current is flowing.

The magnet requires 9 amperes for a field of 1100, orested, the power supply of the magnet is capable of providing 15 amp at 60 volts, obtained from a bridge type metal rectifier circuit. The current in the main coil can be easily controlled by a variac feeding in the primary of the step down transformer, the secondary of which is connected to the rectifier circuit. A filter circuit consisting of a choke of 35 mh and a capacitor of 850 μF reduces the ripple current to 0.1% in the main coil. The field of the magnet is stabilized to a value of 1 part in 1000, by providing a compensating field, which can compensate for a change of $\pm$ 10% in the uniform field.

The performance of the magnet, viz the variation of the field along the radius, and the hystersis property are shown in fig.(10) and fig.(12) respectively.

~~III-5(a)~~

Measurement of the magnetic field gradient was performed as given in III-4(ii)(f). The measurements were carried out for various values of the main coil current. It was found that the gradient was nearly the same for

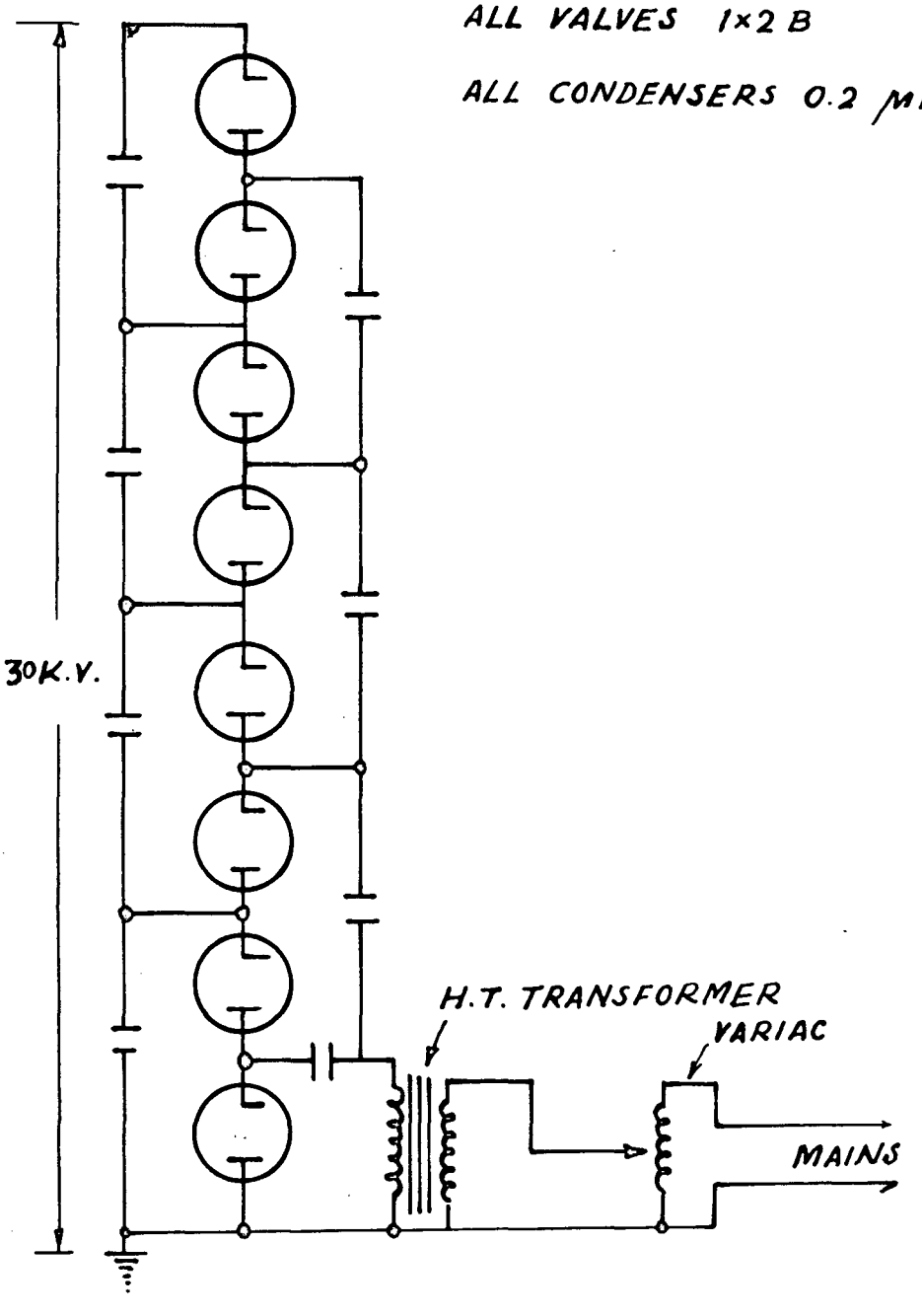

FIG. 13. 30 K.V. UNIT OPERATING ON MAINS FREQUENCY. (50 c/s)

currents upto 4 amperes. The absolute value of the magnetic field was measured by a search coil (calibrated with a standard inductance) along with a ballistic galvanometer. The search coil, had 8222 turns and an average diameter of 1 cm. The field measurement could be checked several times during the course of a run, and further with the NMR measurement of the standard Cs^{137} 624 keV line. The possible error in the measurement of the magnetic field was estimated to be $\sim \pm 0.5\%$.

III-6(i) <u>High voltage unit</u>:

Fig.(13) shows the circuit arrangement of the power supply which is operated at mains frequency. A voltage transformer capable of giving 10 kV. output at 230 volts input was fed from a variac which enables the output voltage to be varied continuously. The rectifier tubes 1 X 2B, were used, which were of the directly heated type and could stand a peak inverse voltage of 28 kV. Thus, these tubes are capable of rectifying upto 12 kV, leaving a safety factor of 20%. The condensers were of 0.2 μF, 8 kV. ratings. It was decided to use 8 stages of voltage doubling to obtain 32 kV. in the final stage, leaving a sufficient safety factor. It was also decided to provide a load, mainly of the voltmeter probe which would take a load current $I_t \sim 10^2 \mu$A at 32 kV. The condensers and the values were mounted on an ebonite board 62cm X 46cm X 0.6cm.

The input terminals to the rectifier and voltage multiplier circuit were fixed in a perspex sheet. This was mounted over the ebonite base in such a way that one thick perspex sheet could be placed between the terminals so as to insulate them from each other and also from the ebonite.

The output terminals were also made in the same manner. The ebonite sheet was supported over a wooden frame work and the filament transformers were placed in the space below the sheet. Each filament transformer had to stand a high voltage of about 16 kV and it was, therefore, immersed in oil contained in plastic boxes. These boxes were sealed with wax so as to prevent any contact of oil with the atmosphere. The output voltage of a practical cock roft walton rectifier is(55)

$$V_{ac} = V_o \left(\frac{C_s}{C}\right)^{-1/2} \text{TANH} \left\{ n \left(\frac{C_s}{C}\right)^{1/2} \cos\theta \right\} - \left[\frac{n^3}{12} + \frac{3n^2}{16}\right] \frac{I_L}{2\pi f C} \quad \cdots (35)$$

where V_{ac} = is output D.C. voltage = 32 kV.

V_o = is input peak voltage.

C_s = is the diode capacitance = $2.5 \times 10^{-12} \mu F$.

n = is the number of stages = 8.

C = is the capacity of each stage = $0.2 \mu F$.

I_L = is the load current = $100 \mu A$mp.

f = is the frequency of A.C.

θ = is the angle of flow of current = 0^o

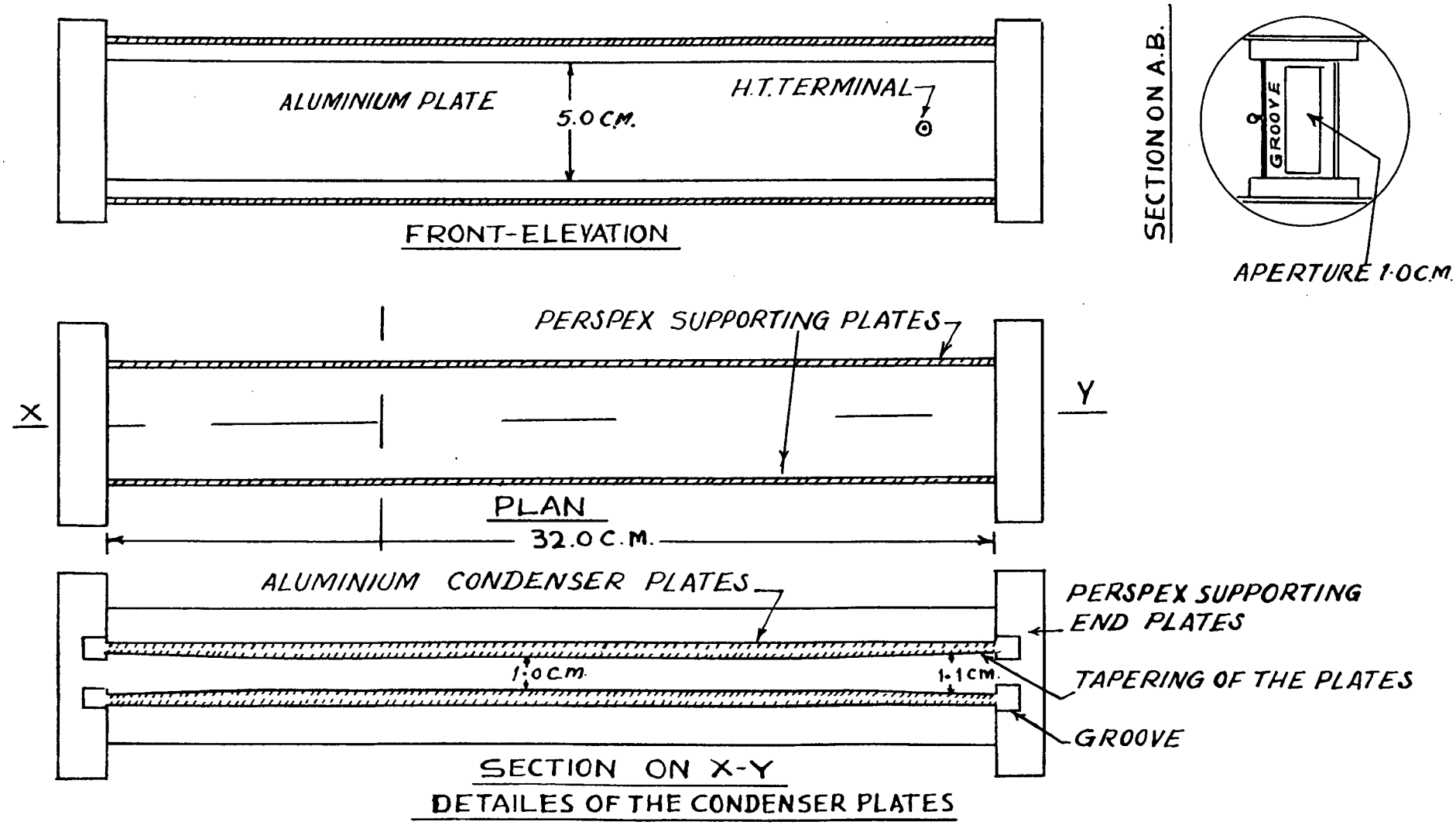

FIG. 14 PLAN ELEVATION & SECTION OF THE CONDENSER PLATE ASSEMBLY

substituting these values one gets $V_c = 5{\cdot}7$ kV. Ripple voltage is given by

$$\delta V = V_0 \left[1 - \frac{1}{\cosh \left[n \left(\frac{cs}{c} \right)^{1/2} \right]} \right] + \left(\frac{n^2}{8} + \frac{n}{4} \right) \frac{It}{fc} \quad \cdots (36)$$

substituting for the above values, ripple factor obtained is about $\pm$ 2%.

[illegible]

The measurement of the electric field was done by measuring the voltage across the condenser plates by a 300 MΩ probe along with a micro-ammeter, so that 300 volts corresponded to a current 1 μA. Thus, the electric field was measured to an accuracy of $\pm$ 1%.

III-7. <u>The Condenser Plates</u>:

The condenser plates, of aluminium, 32cm X 5cm X 0.5cm were highly polished and tapered at the ends as stated on page 49. They are fixed in the perspex frame work (see plate and fig.14). The perspex also serves as a good insulator. The plates are adjusted in the grooves parallel to each other, and set firmly by the use of araldite. The high voltage terminals, were soldered and then araldite was pest over it to avoid leakage, by forming a smooth insulating surface. The perspex frame work was then housed in an alkathene pipe and was fixed in position, so that

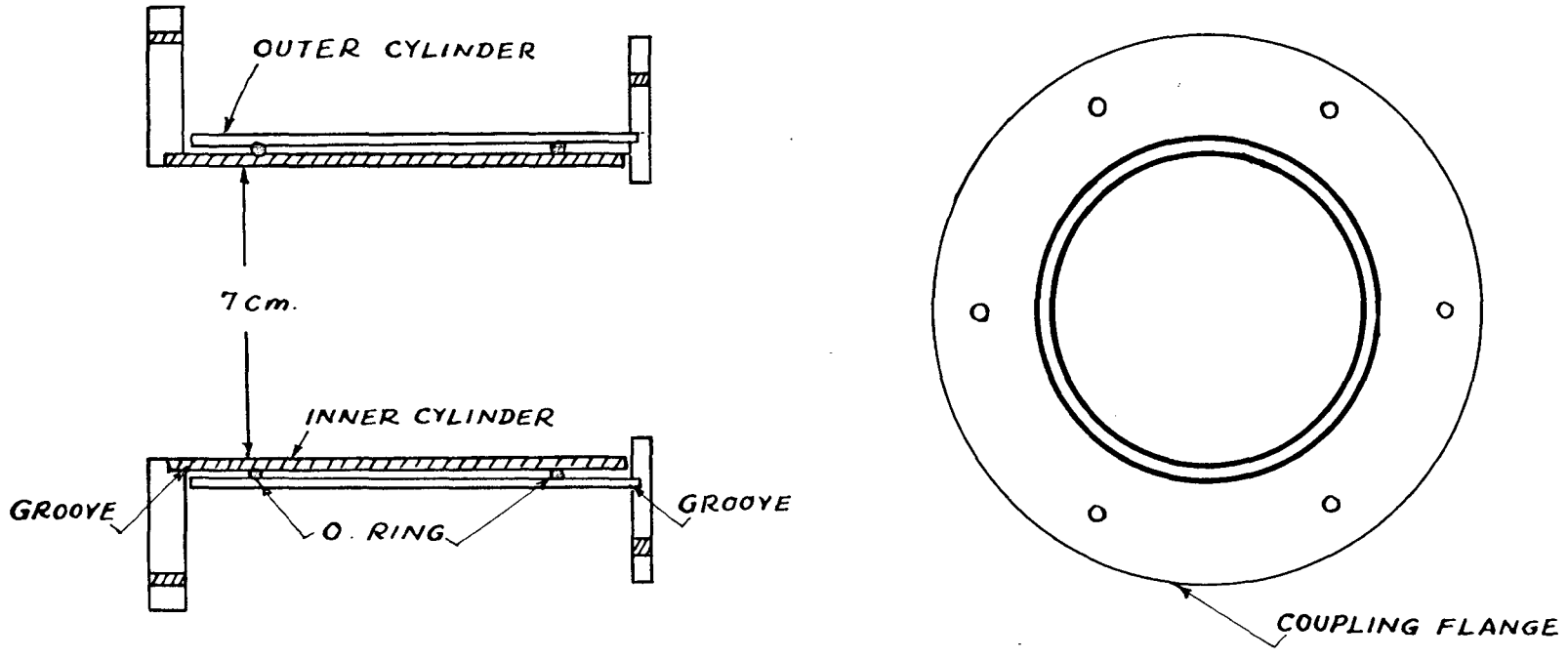

FIG. 15 ROTATING SEAL ARRANGEMENT

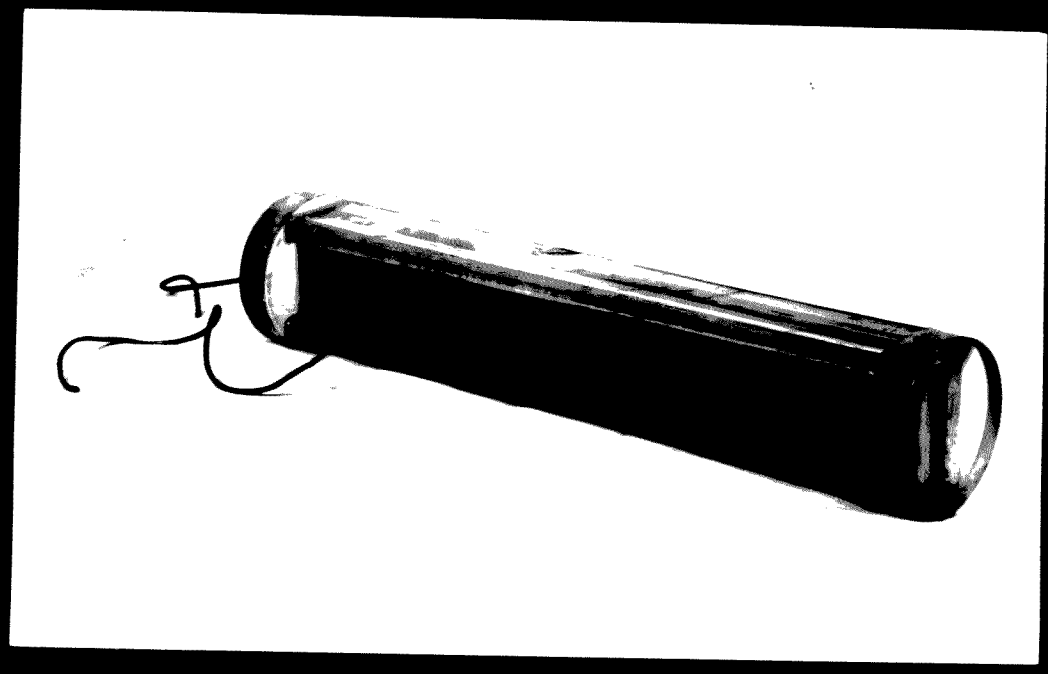

The Condenser late Assembly

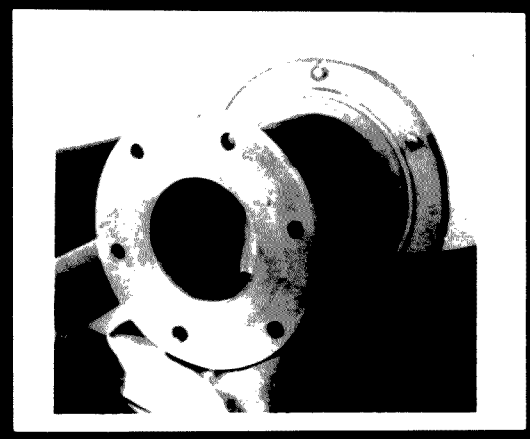

The Rotating Seal Arrangement

the condenser plates are symmetrically placed in the centre of the pole pieces of the magnet. The high voltage terminals were connected to the plates through the alkathene pipe. The plan, elevation, and section of this assembly is shown in fig.(14).

III-8. Rotating Seal Arrangement:

The Wien-filter was coupled to the scattering chamber, through a rotating seal arrangement consisting of two concentric brass cylinders. (see plate and fig.15). The inner cylinder has two 'O' rings, fixed in the grooves, the outer cylinder slides firmly yet easily over the inner one, without disturbing the vacuum. The cylinders were coupled to the Wien-filter and scattering chamber, through perspex flanges.

III-9. The Scattering Chamber: was constructed by a double T joint made from alkathene pipes of diameter 4 inches, as shown in fig.(8). At the joint, another small piece of the same pipe was welded, in the vertical position through which the foil was inserted in the beam.

The whole of the scattering chamber was fixed firmly on a wooden stand, made of two pillers with a circular bracket for the pipe. The base had leveling screw's for the beam alignment. The rotation of the chamber was made regular and smooth by having a ball-bearing arrangement in the circular bracket.

III-10. The Scintillation Counter Detector Probe:

Two identical NE 102 A plastic scintillators of 5 cm diameter and 4 mm thick were highly polished by alumina. Thin aluminium foil (.00025") was glued on the scintillator surfaces. These were coupled optically to the photomultiplier (EM 9714), by the silicone cement and were covered by the brass mask having an opening of suitable diameter.

The two photomultipliers were enclosed in iron cylinder for magnetic shielding. These were placed symmetrically (at a distance of 5 cm from the beam) with respect to the beam axis, inside the alkathene pipe and were prevented from sliding from their position by having perspex stops. The light produced in the scintillators was collected by the photo cathodes of the photomultipliers, whose output after amplification and pulse height selection was scaled by a decade scaler. The photomultiplier was run at a suitable voltage (1500 v) so as to provide the optimum gain and signal to noise ratio. The tube dynode potentials were supplied by a 30 MΩ potentiometer chain; the voltage across which could be varied from 1.5 kV. to 2.5 kV. The pulses from the photomultiplier tubes were fed via the cathode follower to an A.E.E.T. non overload linear amplifier. The amplified pulses were passed through a single channel pulse height analyzer. The selected

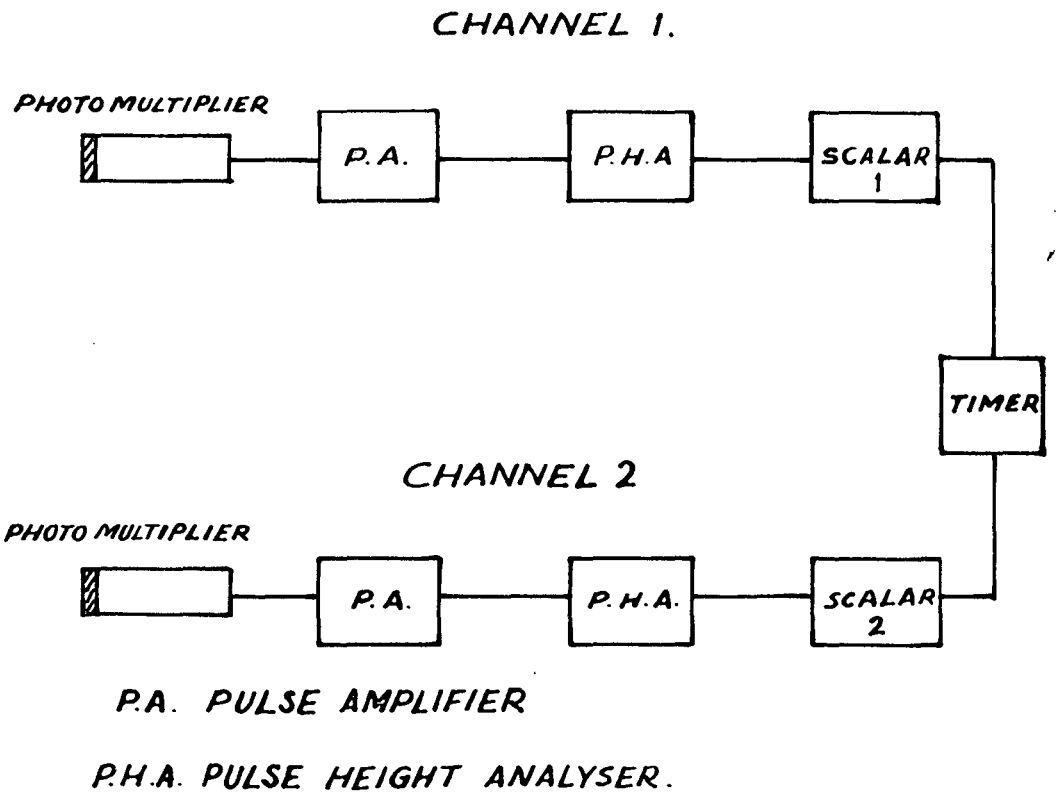

FIG. 16 BLOCK DIAGRAM OF THE ELECTRONICS

The Scattering Foil Holder

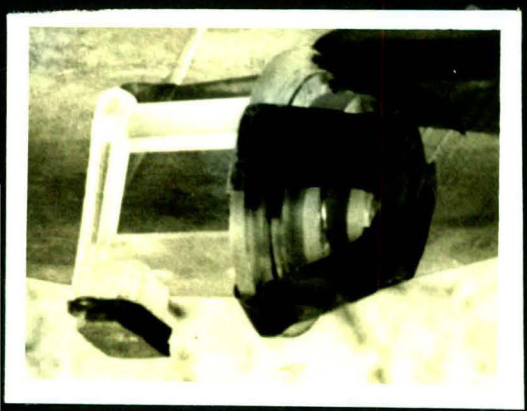

The Source Holder

pulses were fed into a scaler to measure the singles counting rate in individual channels. A block diagram is shown in fig.(16).

III-11. Beta-sources, Source Holder, Scattering Foil and Foil Holder:

It was decided to have a pure beta source, so that no gamma background is present, which effectively reduces the secondary electrons, the wall scattering etc, and, thus, the disadvantage usually associated with a Wien-filter (when working with a gamma source) because of its straight line geometry, is not there. Thallium was deposited uniformly on mylar over a circular area of diameter 1 cm. The thickness of the source was found by weighing on a micro-balance, to be $3 \sim 4$ mg/cm^2. The source holder is made of plexi-glass (perspex) and is shown in plate

Au-gold foils of thicknesses 500μg/cm^2 to 1000μg/Sq.cm^2 were prepared$^+$ by vacuum evaporation of the pure gold (99.9%) on cellulose backing. The masses were found by weighing on a microbalance, before and after deposition, to an accuracy of 1.(1%) The foil holder is made of a perspex frame fixed to an aluminium rod, as shown in plate

---

$^+$ The author is obliged to the Director N.C.L. Poona for facilities provided for preparing gold foils.

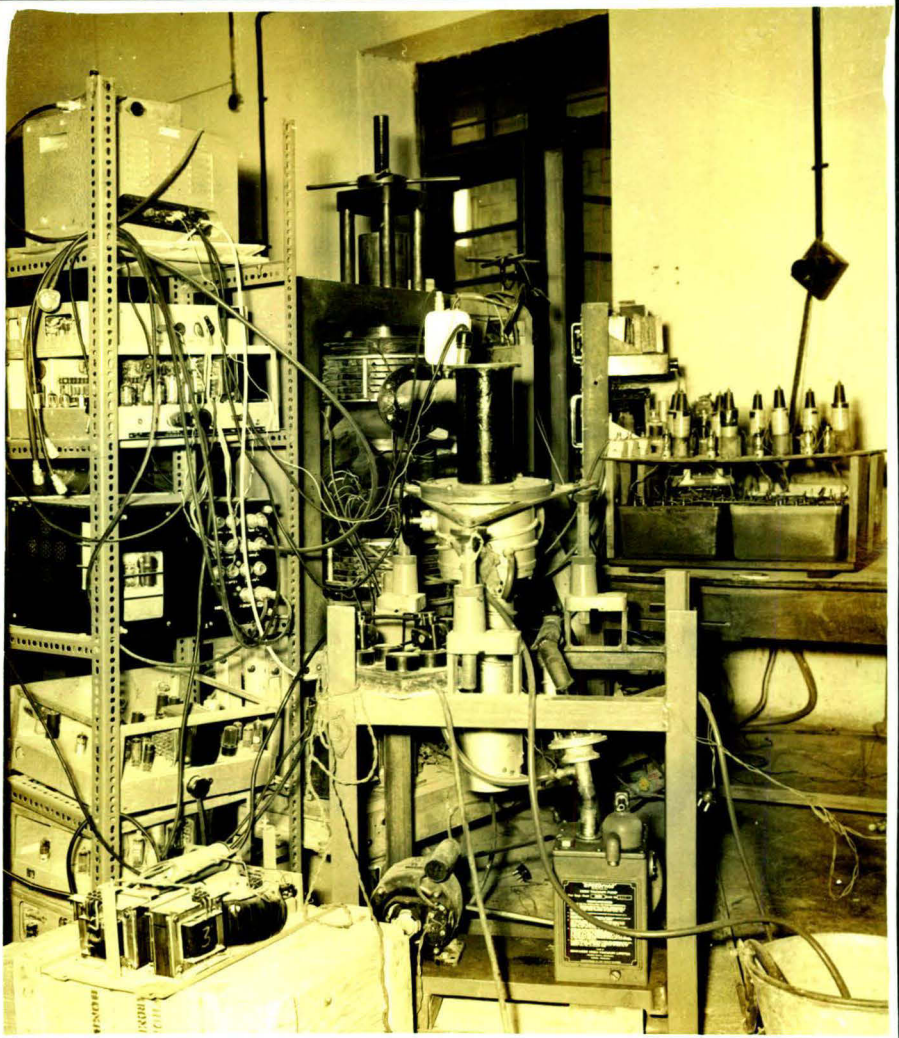

The back view of the experimental set-up showing the vacuum system and the high voltage unit.

The foil holder can be pushed inside the beam from outside without disturbing the vacuum through a sliding 'O' ring arrangement. The foil can also be rotated about the beam axis.

III-12. The Vacuum System used in this experiment was mounted on a trolley. It consisted of a 4" oil diffusion pump supplied by the Technical Physics Division of the Atomic Energy Establishment, Trombay. This was backed by a Hindustan 2 stage 150/2s rotating pump. This combination was sufficient to reduce the pressure in the scattering chamber to about 10^{-4} mm in about 30 minutes. An indication of the pressure in the system was provided by a combined Pirani and Penning gauge.

The check runs, the procedure for taking the experimental measurement, the performance of the equipment and the result are described in Chapter IV.

CHAPTER IV

PERFORMANCE OF THE WIEN-FILTER AND STATEMENT OF RESULTS

IV-1. Performance Of The Wien-filter:

After having described the construction of the main parts of the equipment, its performance so far as the horizontal spread of the beam, resolution, linearity, and transmission etc. are concerned are now described.

IV-1(i) The horizontal spread of the beam, at the foil position, which is at the centre of the scattering chamber, was measured by a beam scanning arrangement. A pure beta source Tl^{204} was placed in the source holder, which also provides primary collimation of the emerging electron beam. The whole system was evacuated to a pressure better than 10^{-4} mm. By applying precalculated values of electric (E) and magnetic fields (B) to the condenser plates, a beam of electrons of energy $E/B = v/c \simeq 0.6$ was selected, from the continuous beta spectrum of Tl^{204}. The beam was scanned by a scintillation counter probe, which consisted of a plastic NE 102 scintillator covered by a slit 2 mm wide. The detector was moved horizontally through successive distances of 2 mm. each by a vacuum movement worked from outside. The brass pipe holding the scintillator probe could be easily inserted in the vacuum

FIG. 17 HORIZONTAL BEAM PROFILE

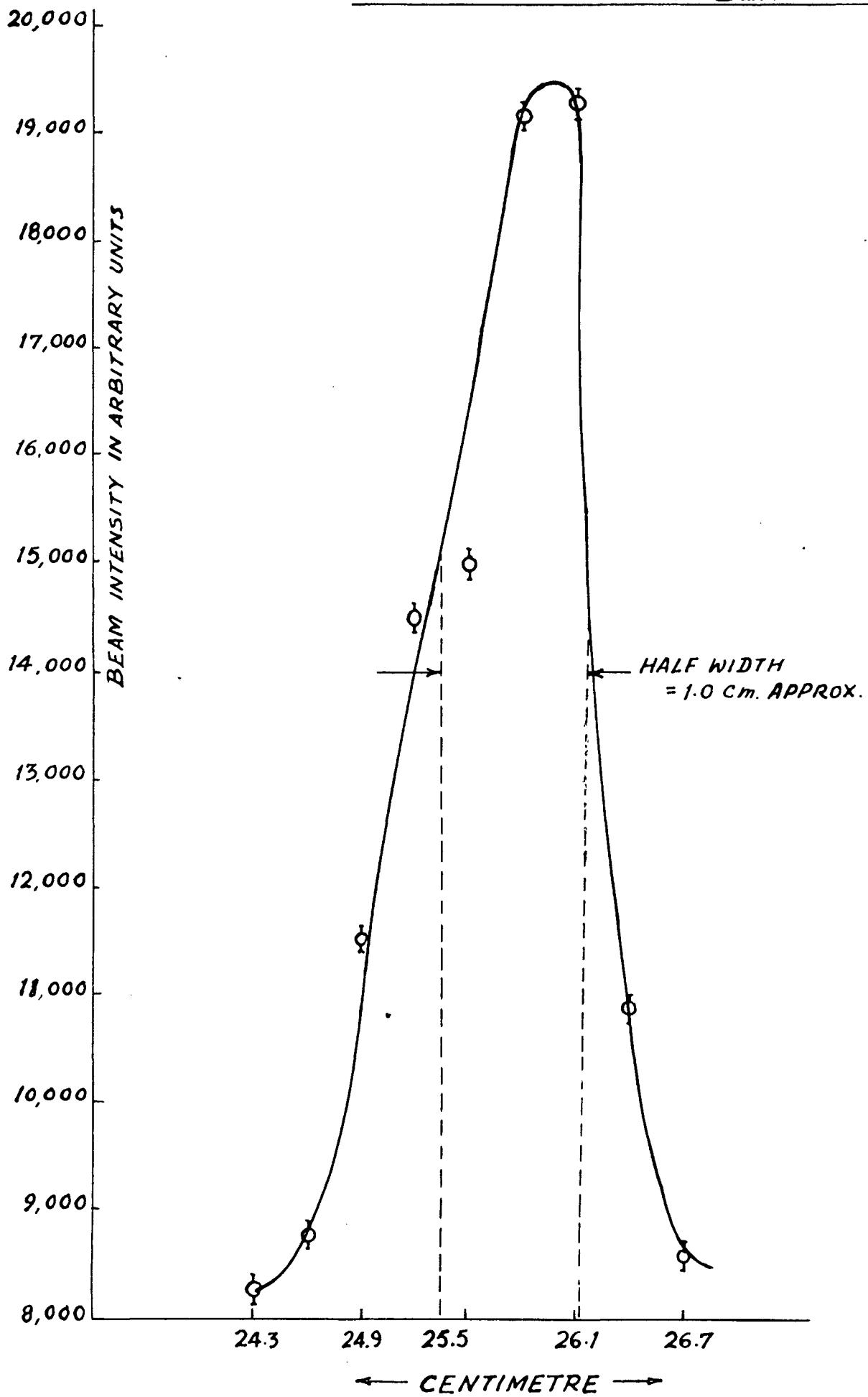

chamber through two 'O' ring seals. It was possible to move the probe over the rings without disturbing the vacuum of the order of 0.1 micron. The movement of the probe could be controlled to better than half a millimetre. Once the position of the probe was adjusted, it could be held in that position by tightening a collar through which the probe passed. The electron flux was measured at each position of the detector slit on both sides of the beam axis. The results of these measurements are given in table 4 and are plotted in fig.(17).

Table 4

Horizontal distribution of the incident beam flux.

Position of the detector slit in arbitrary units.	Counting rate after subtracting the background.
24.3	250
24.6	750
24.9	3500
25.2	6500
25.5	7000
25.8	11250
26.1	11300
26.4	3000
26.7	500

It will be seen from the figure that the beam has a spread of 2 cm (half width 1 cm) where the intensity

FIG. 18. BETA SPECTRUM OF Tl^{204} BY WIEN-FILTER

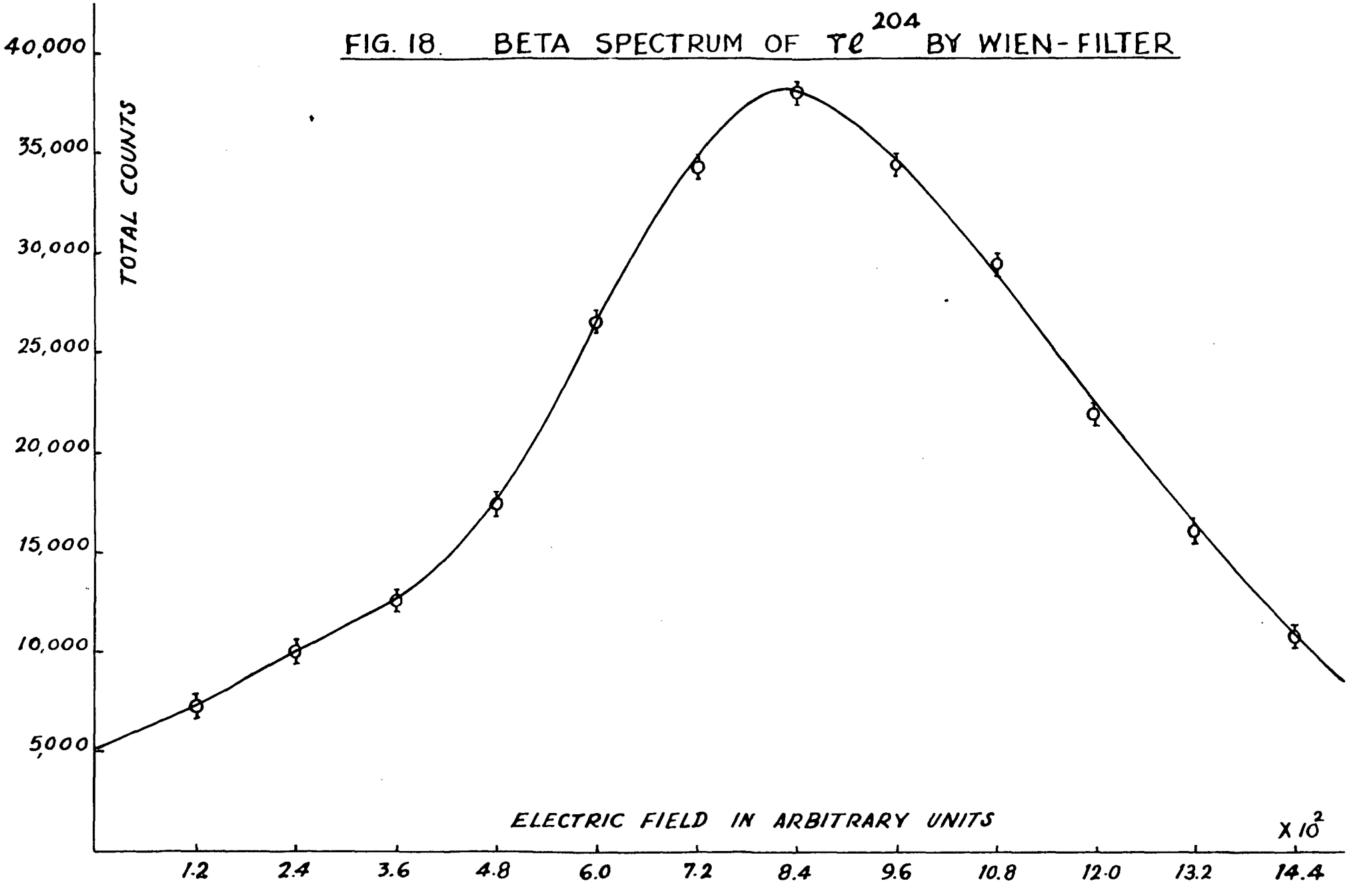

drops down to 1/20th of its intensity at the centre. Also the beam is mostly symmetrical about the axis of the beam, thereby indicating that the alignment of the Wien-filter and the scattering chamber was achieved satisfactorily.

IV-1(ii) Continuous beta spectrum of Tl^{204} :

From the horizontal scan of the beam, the position of the maximum beam intensity was determined. The detector was placed in this position. A pre-calculated magnetic field was applied and kept constant while the energy spectrum of the beta particles was swept over the scintillator probe by merely altering the electric field, from zero to a sufficiently high value till the counting rate had fallen down sufficiently after passing through the peak value of the energy distribution. Thus, electrons of continuously increasing energy (according to $E/B = v/c$) values are detected, giving a continuous beta spectrum. The amplification was selected in such a manner that the ratio of signal to noise was maximum at a certain suitably chosen value of the bias voltage. The spectrum was repeated for different values of the constant magnetic fields.

A typical result is given in the table 5 and plotted in fig.(18). The counting time was sufficiently long to give a good statistics giving the error on this account of about $1 \simeq 2\%$.

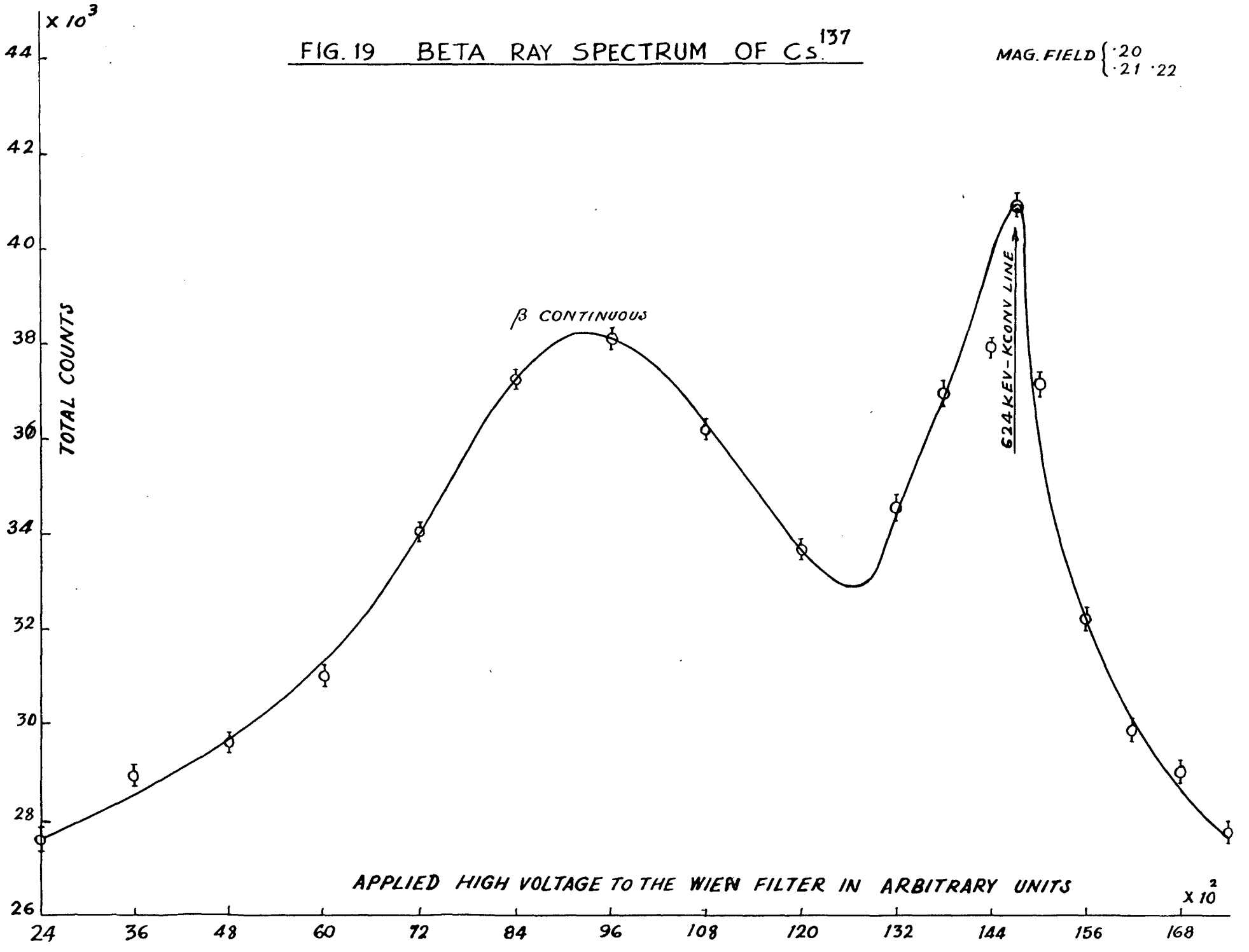
FIG. 19 BETA RAY SPECTRUM OF Cs 137
MAG. FIELD ·20 ·21 ·22
X 10 3
TOTAL COUNTS
44
42
40
38
36
34
32
30
28
26
β CONTINUOUS
624 KEV - K CONV LINE
APPLIED HIGH VOLTAGE TO THE WIEN FILTER IN ARBITRARY UNITS
X 10 2
24
36
48
60
72
84
96
108
120
132
144
156
168

Table 5

Magnetic field ≃ 20 oersted

Electric field in kV/cm.	Counting rate.
0	5,000
1.2	7,500
2.4	10,000
3.6	12,500
4.8	17,500
6.0	27,500
7.2	34,000
8.4	38,000
9.6	34,000
10.8	28,000
12.0	22,000
13.2	16,120
14.4	11,500

IV-1(iii) Continuous beta spectrum of Cs^{137}:

The beta spectrum of Cs^{137} was also studied using this Wien-filter. The value of the magnetic field was so fixed that the electric field required for 624 Kev conversion line, was well below the maximum value of E, which, one could apply before a possible corona discharge becomes rather more frequent. The spectrum was repeated for different values of magnetic fields. One of such results is given in table 6 and is shown in fig.(19).

It will be seen from this figure that the continuous beta spectrum peak and the conversion line peak have been resolved. And the theoretical ratio of the energies of the two peaks viz 2 was obtained experimentally also.

The position of the conversion line peak is at 14.4 kV, which agrees well with the theoretical value calculated from v/c = E/B for 624 kev. The difference can be explained as due to the finite resolution of the Wien-filter. The gamma background was subtracted to give the electron flux at different electric field values.

Table 6

Applied voltage in kV.	Counting rate.
2.4	27,550
3.6	28,400
4.8	29,500
6.0	31,000
7.2	34,000
8.4	37,000
9.6	38,200
10.8	36,250
12.0	33,700
13.2	34,500
14.4	37,800
15.0	41,000
15.6	35,500
16.8	29,500
18.0	27,800

IV-1(iv) Resolution of the Wien-filter from pulse height spectrum of Cs^{137} :

The pulse height spectrum of Cs^{137} at the conversion line peak was obtained by selecting the amplification and H.T. such that the conversion line peak was obtained at a bias voltage well above the thermal noise level and well below the saturation level of the amplifier.

FIG. 20 PULSE HEIGHT SPECTRUM OF Cs^{137}

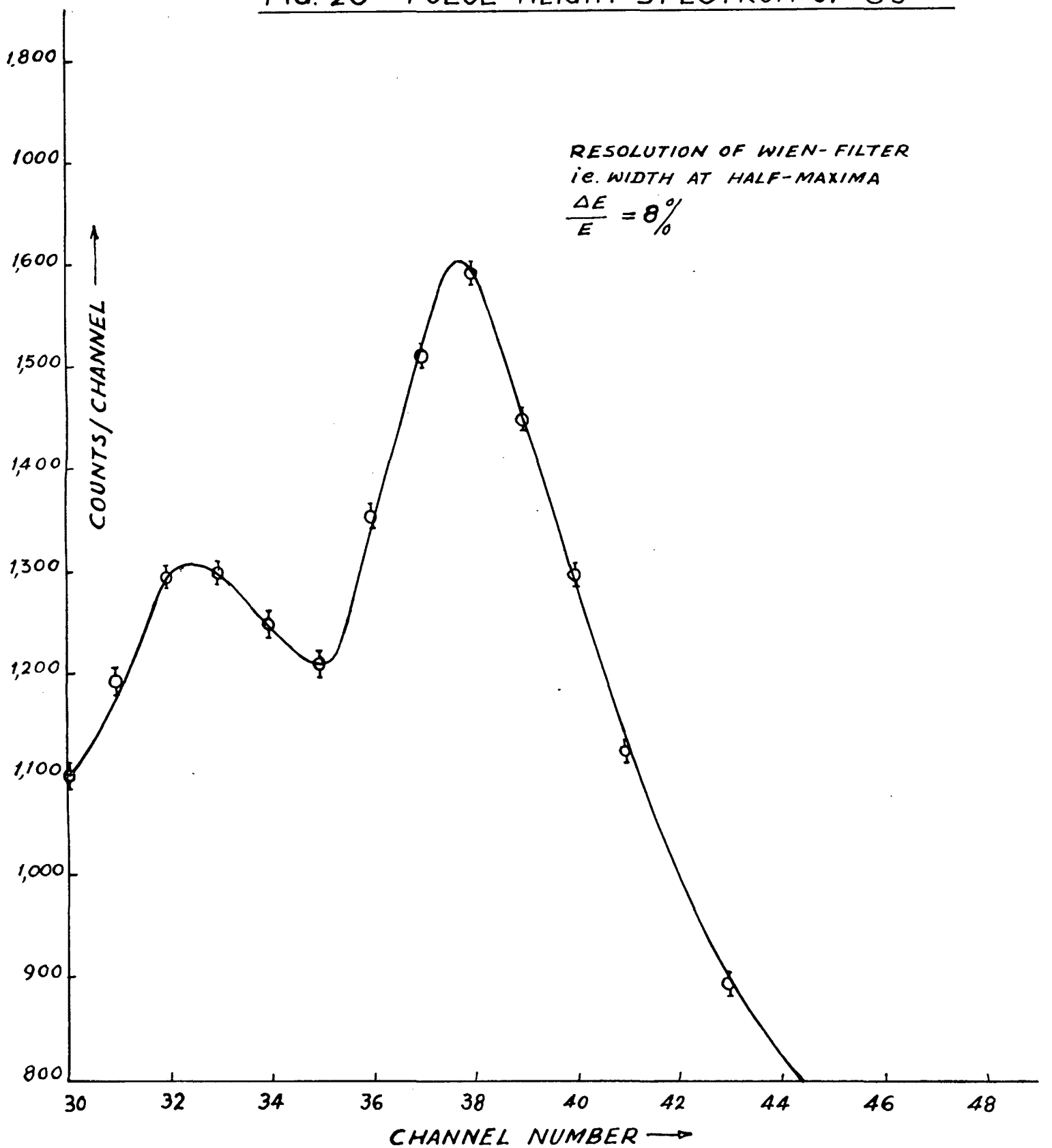

First the gamma pulse height spectrum was observed by removing all the electrons from the beam after applying a very high magnetic field, then it was subtracted from the β-γ pulse height spectrum, to have only beta pulse height spectrum of Cs^{137}. The electric and magnetic field values were selected so that $E/B = v/c \simeq 0.9$ = 661 kev.

The peak was obtained at the 38 volt channel for amplification of 80 and H.T. = 1500 volts. The resolution was calculated from width at half maximum, $\frac{\Delta E}{E}$ % which is about $\pm$ 8%. The results of this measurement are given in table 7 and are plotted in fig.(20):

Table 7

Channel number width 1 volt.	Counts/channel
30	300
31	375
32	500
33	500
34	450
35	400
36	550
37	700
38	800
39	650
40	500
41	325

IV-1(v)The calibration & linearity of the detecting system:

The detecting system was calibrated and its linearity tested by Cs^{137} 624 kev conversion line. The magnetic field applied was such that the required electric

FIG. 21 624 Kev CONVERSION LINE SPECTRUM FOR TWO VALUES OF MAGNETIC FIELD SHOWING THE LINEARITY OF THE WIEN-FILTER

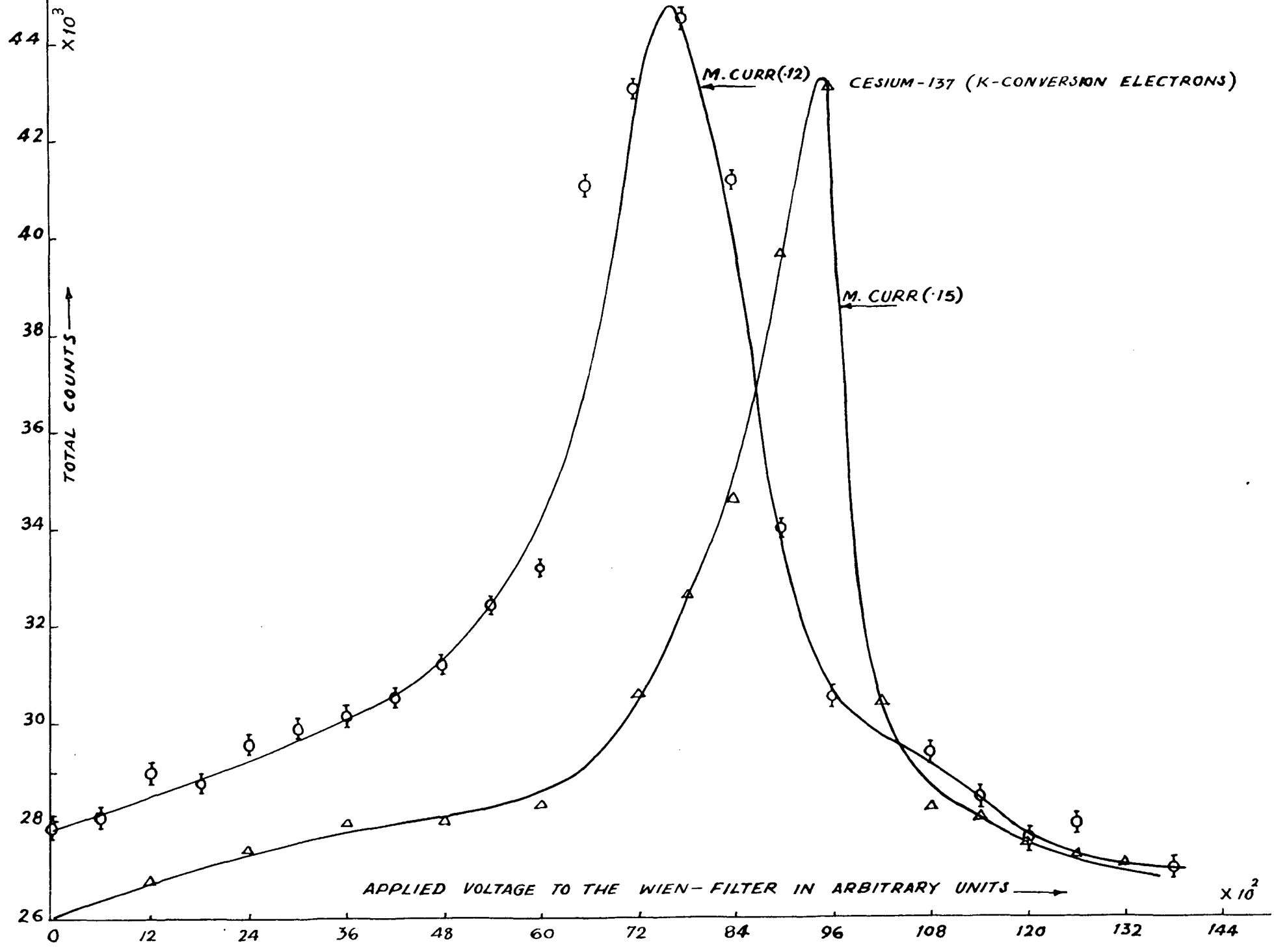

field [E = B x v/c (0.9) x 300 volts/cm] was below the maximum value, before a discharge takes place, then the electric field was varied from zero onward to obtain the conversion line peak. The process was repeated for different values of magnetic fields, and it was found that the peak position (electric field required) shifts in the same ratio as that of the magnetic field, thus giving same $E/B \simeq v/c = 0.9$ which is expected as the conversion line energy is constant. Also the system gets calibrated automatically as the energy (v/c) of the conversion line being known, the value of the required magnetic field B could be calculated from $E/B = v/c \simeq 0.9$, knowing the electric field E required for the peak. It was found that the calculated value B of magnetic field β agreed very well with the absolutely measured value using a search coil. The results are given in table 8 and are plotted in fig.(21).

Table 8

Magnetic field in terms of main coil current 0.12 amperes.		Magnetic field in terms of main coil current 0.15 amp.	
Electric field in kV/cm.	Counting rate.	Electric field in kV/vm	Counting rate
0	28,000	0	26,000
1.2	29,000	1.2	26,500
2.4	29,750	2.4	27,500
3.6	30,000	3.6	28,000
4.8	31,020	4.8	28,000
6.0	33,000	6.0	28,500
7.2	43,000	7.2	30,500
7.8	44,500	8.4	34,500
8.4	41,000	9.0	39,500
9.0	34,000	9.6	43,000
9.6	30,250	10.2	30,500
10.8	29,000	10.8	28,500
12.0	27,750	12.0	27,500

IV-2. Setting of The Two Channels For Observing The L-R Asymmetry:

IV-2(i): The linearity of the two pulse height analyzers along with the amplifiers was tested before the two channels were equalized. A beam of electrons from Tl^{204} of energy approximately the same for which the L-R asymmetry measurements were carried out was selected by applying proper values of electric and magnetic fields.

The pulse height peaks of Tl^{204} electrons were observed for amplification factors 40 and 56. It was found that the peak position shifted nearly in the same ratio as the amplification factor.

It was also observed that the peak becomes more flat and of less height as the amplification increases, which could be explained by the fact that the electrons get distributed over a number of channels as the amplification increases. It is seen that the peak positions in the two channels for amplification factor 40, lie within a difference of 1 volt.

These results are given in table 9 and 10 and are plotted in fig.(22) for the right channel.

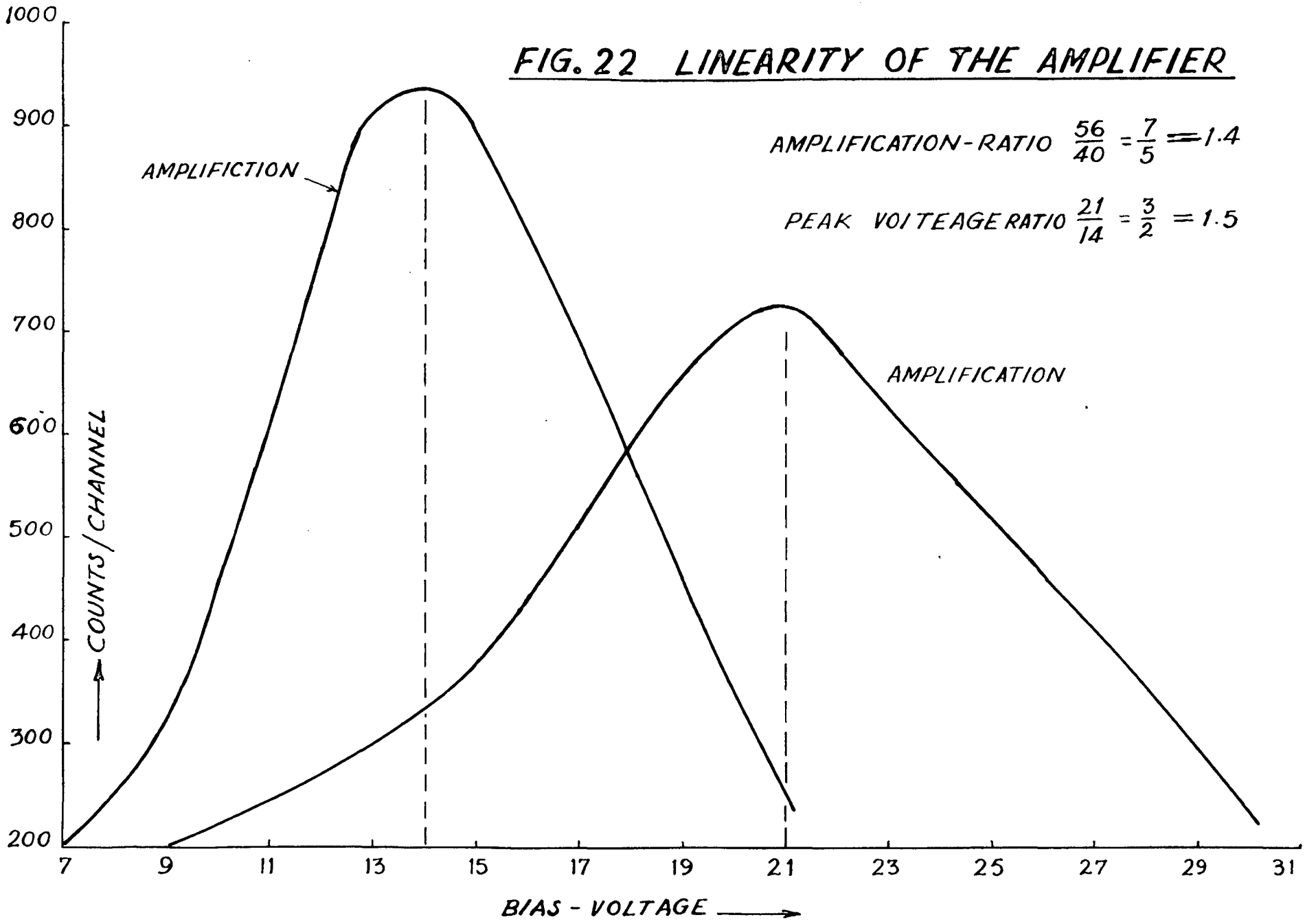
FIG. 22 LINEARITY OF THE AMPLIFIER
AMPLIFICATION-RATIO $\frac{56}{40} = \frac{7}{5} = 1.4$
PEAK VOLTAGE RATIO $\frac{21}{14} = \frac{3}{2} = 1.5$
AMPLIFICTION
AMPLIFICATION
COUNTS/CHANNEL
1000
900
800
700
600
500
400
300
200
7
9
11
13
15
17
19
21
23
25
27
29
31
BIAS - VOLTAGE

Table 9 : Right Channel

Amplification 40		Amplification 56	
Bias voltage.	Counts/channel.	Bias voltage.	Counts/channel
7	200	9	200
9	325	11	250
11	600	13	300
13	920	15	375
14	940	17	500
15	900	19	650
17	700	21	725
19	425	23	600
21	250	25	550
		27	425
		29	300

Table 10 : Left Channel

Amplification 40		Amplification 56	
Bias volt.	Counts/channel.	Bias volt.	Counts/channel
9	194	9	134
11	246	11	139
13	419	13	
15	702	15	205
17	615	17	230
19	429	19	319
21	283	21	
23	219	23	432
		25	461
		27	380
		29	290
		31	170

FIG. 23 PULSE HEIGHT SPECTRA OF TH 204 ELECTRONS OF SAME ENERGY AS RECORDED BY THE TWO CHANNELS

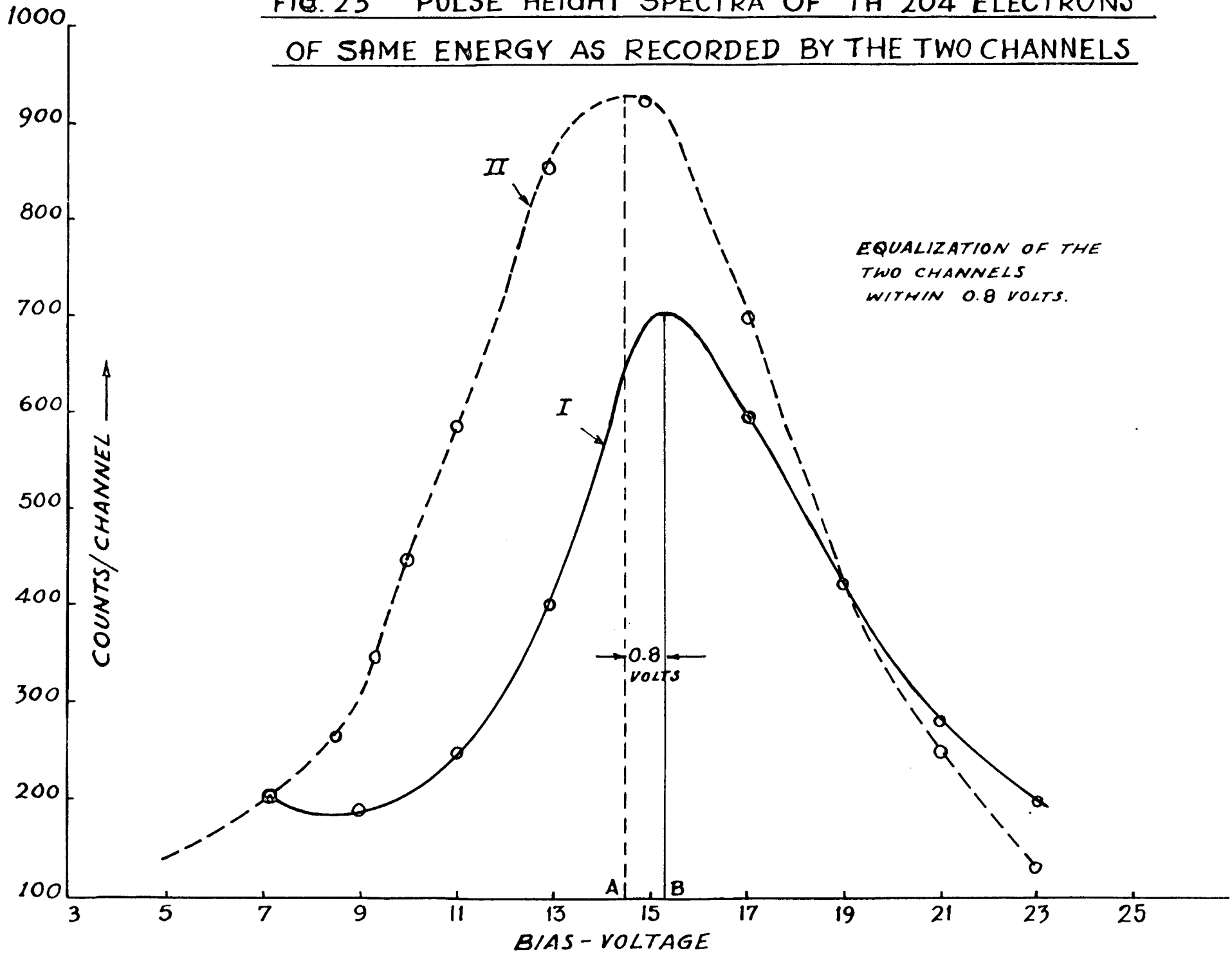

IV-2(ii) Equalization of the two detecting systems:

Before one proceeds to carry out the left-right asymmetry measurements, it is very essential to have the two systems as identical as possible. The two should be set in such a way that they record the same energy peak nearly at the same pulse height channel. The two systems were, thus, equalized by proper adjustment of the amplification factor, and the H.T. voltage applied to the photomultiplier tubes. The energy selected was of the same value as the one required for the asymmetry measurements. The amplification was so selected to have signal to noise ratio as large as possible for the above energy. It will be seen from the figure that the peak position in the two channels differed by only 0.8 volt, which was well within the accuracy of the channel width adjustment possible with our equipment. These results are given in tables 9 and 10 and are plotted in fig (23).

IV-2(iii) Pulse height spectrum of $T\ell^{204}$ of beta value $v/c \simeq 0.6$ as was selected by the Wien-filter before it was incident on the gold foil, was obtained by applying proper values of electric and magnetic fields.

It was also observed further that after scattering, the pulse height spectrum peak of scattered electrons was shifted by about 2-3 volts to a lower channel number. Before scattering the peak was at 11 volts while, after

FIG. 24 PULSE HEIGHT SPECTRUM OF Th^{204} OF DIRECT AND SCATERED BEAM

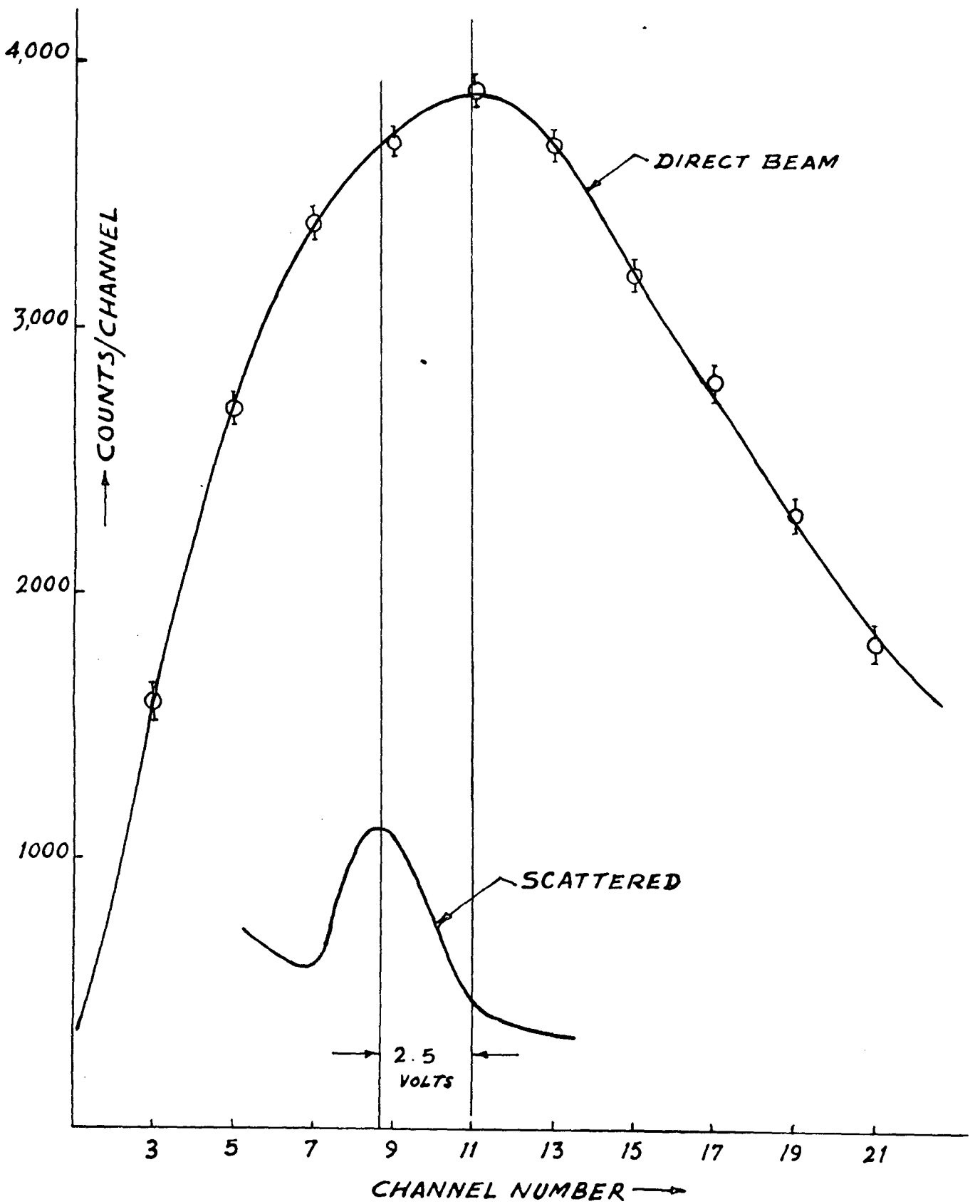

scattering it was observed to lie between 8-9 volts. The intensity after scattering drops down sufficiently as is expected. These results are given in table 11 and are plotted in fig (24).

Table 11

Before scattering		After scattering	
Channel number.	Counts/channel.	Channel number.	Counts/channel
3	1600		
5	2700	6	650
7	3400	7	600
9	3700	8	880
11	3900	9	1070
13	3700	10	890
15	3200	11	480
17	2800	12	340
19	2300	13	400
21	1800	14	400
		15	

IV-3. Measurement Of The L-R Asymmetry And The Observed Value Of Polarization For Tl^{204}, Electrons Of $v/c \simeq 0.6$

After setting the two detecting systems identical and knowing the nature of the pulse height spectra of the incident electrons and those scattered by the gold foil, the intensities of the scattered electrons on the left and right side of the beam were measured, and L-R asymmetry calculated. The scattered electrons were counted for a

long time interval to improve the statistical accuracy. These measurements were carried out for two Au foils of different thicknesses (t). The foil was inclined at 60^{o} to the beam axis. Also the reflection transmission effect, and instrumental asymmetry effects ($0-180^{o}$ position), were tested. The L-R asymmetry was observed for different azimuthal angles from $0-180^{o}$ position onwards, to $90-270^{o}$ position. The counters were also rotated by 180^{o}. The background observed before introducing the foil was subtracted from the I_L and I_R intensities observed after the foil was introduced: several runs were taken, the typical one is reported in table 12.

Results: For $Te^{204} \xrightarrow{\tilde{\beta}} Pb^{204}(\bar{2} \rightarrow \overset{+}{0})$ (unique, first forbidden).

The value of the longitudinal polarization P_ℓ was calculated from $P_\ell = \frac{\Delta}{(v/c)\, S(\theta)}$ where Δ is the observed L-R asymmetry and $S(\theta)$ is the asymmetry function, the value $S(\theta)$ taken from D.F. Nelson and Pidds (61) data is

0.274 ± 0.008 for Au, and for $v/c \simeq 0.6$ for $\theta = 90^{o}$

Δ observed $\simeq 0.18$

hence the value of polarization $P_\ell = -(1.09 \pm 0.083)\, v/c$ which is in agreement with the predicted value.

Table 12

L-R-Asymmetry measurements for Tl^{204} electrons of $v/c \simeq 0.6$ for transitions $Tl^{204} \xrightarrow{\beta^-} Pb^{204}$ ($\bar{2} \rightarrow 0^+$) (unique first forbidden)

E = 14.4 kev/cm B $\simeq$ 76 oersteds.

Source thickness T $\simeq$ 3 mg/sq.cm

Ist Foil t = 0.5 mg/sq.cm

0° I_L - Counts.	180° I_R - Counts.	90° I_L - Counts.	270° I_R - Counts	
1900	1825	2800	1900	Reflection
		2820	1850	Transmission
		2810	1875	Mean

(After subtracting the geometrical asymmetry)

$$\Delta = \frac{I_L - I_R}{I_L + I_R} \simeq 0.18$$

II Foil t $\simeq$ 1 mg/sq.cm

0° I_L - Counts.	180° I_R - Counts.	90° I_L - Counts.	270° I_R - Counts.	
1850	1925	1800	2750	Reflection
		1900	2850	Transmission
		1850	2800	Mean

(After subtracting the geometrical asymmetry)

$$\Delta = \frac{I_L - I_R}{I_L + I_R} \simeq 0.185$$

After reporting the performance of the equipment (Wien-filter) fabricated by the author, and a preliminary set of observed L-R-asymmetry and the value of polarization P_e for Tl^{204} electrons for $v/c \simeq 0.6$, the discussion of the result, and the conclusions are reported in the last (V) chapter of this thesis.

CHAPTER V

DISCUSSION OF RESULTS AND FUTURE POSSIBILITIES

Numerous papers devoted to the experimental investigation of longitudinal electron polarisation in beta decay have shown that the polarisation is either equal to or negligibly different from v/c for a large number of elements. However, there exist several cases of deviations in which the polarisation differs appreciably from unity (in units of v/c). Apparently, some deviations are strongly correlated with the deviation of the beta spectrum from the Fermi shape(62). There are also other instances, such as Au^{198} (the $2^{+} \longrightarrow \overline{2}$ transition) whose electron polarisation equals unity at energies greater than 200 kev but deviates from unity at low energies (100-150 kev). In order to study these deviations, accurate experiments are very desirable either with conventional apparatus or with new ideas.

The results obtained with the present apparatus were stated in Chapter IV.

The data obtained require certain corrections discussed below.

V-1(4) Plural and multiple scattering in the target:

This contribution is the most important source of error in Mott scattering. Plural scattering consists of

two scattering events of about equal angle; multiple scattering consists of a succession of small-angle scattering. Both effects contribute to the counting rate in the detectors C_L and C_R. In either case, the individual scattering event will involve angles of less than, say 60^o, then $S(\theta < 60^o)$ is nearly zero. The contribution from plural and multiple scattering, thus, does not show an asymmetry, and it must be subtracted from the total counting rate in order to find true assymetry L/R.

The foil can be made thin enough so that the contribution from multiple scattering is very small. It is much more difficult to get rid of plural scattering or to correct for it by calculation. Foils thin enough to eliminate the contribution due to double scattering yield only very low counting rates. Moreover, the ever-present wavyness of very thin foils considerably enhances the contribution of double scattering over the amount expected from theoretical estimates.

For thin targets ($t < 1$ mg/cm^2 even at electron energies of 600 kev) a linear extrapolation is used(43,56). One plots either L/R or $(L-R)/(L+R)$ verses the foil thickness and extrapolates to zero thickness.

An improved approach, which fits the data for a much larger target thickness, is to plot the function

$[PS(\theta)]^{-\frac{1}{2}} = \sqrt{(L+R)/(L-R)}$ verses the target thickness. The extrapolation to zero thickness then yields the desired value of P. As pointed out above this correction can be obtained by extrapolating to zero thickness of scatterer, the inverse of the azimuthal asymmetry obtained from the measurement with different thicknesses of scatterer. However, for the foils used, this correction is not larger in magnitude than the statistical errors, it cannot be determined in this way from the two polarisation values obtained by us with two different thicknesses of scatterer - 500 μg/sq.cm and 1 mg/sq.cm. We have, therefore, followed the method of Alikhanov et al to calculate the contribution δ_o to the azimuthal asymmetry because of multiple scattering from the equation

$$\delta_o = \delta(t) \left[1 + \frac{(0.022 + 0.004)}{(\beta v/c)^2} t \right]$$

which in our case at a mean energy of 128 kev and foil thickness 500 μg/sq.cm has a magnitude of about 2 %, and for a foil of thickness 1 mg/sq.cm , a magnitude of about 3 %. The observed scattering asymmetry is less than that expected for single scattering because of multiple scattering. It is, however, felt that a thorough investigation of the effect of multiple scattering on the azimuthal asymmetry needs a further careful investigation. This could not be done at present because of the limitations in procuring sources deposited in a controlled manner, and

also due to the difficulties in obtaining gold foils of various thicknesses. Nevertheless, for the preliminary investigations reported in this thesis, the approximate magnitudes of the corrections on this account are fairly reliable.

V-2. Depolarization:

The polarization vector of electrons remains approximately fixed with respect to the laboratory system during multiple scattering. More accurately, if the momentum is turned by an angle $\Delta\Psi$ by multiple scattering in low -Z material, then the polarization vector turns only through an angle $\Delta\Phi$, given by

$$\Delta\Phi = \Delta\Psi\left[1-\left\{1-\left(\frac{v}{c}\right)^2\right\}^{-\frac{1}{2}}\right]$$

where v is the velocity of the electron. This effect leads to an energy dependent depolarization of an electron beam. Electrons initially moving in the direction towards the analyzer, i.e. the target or the polarization transformer, suffer no appreciable depolarization. Electrons which initially moved in the directions and are scattered into the acceptance angle of the analyzer have their polarization vector pointing in different directions. Electrons originally moving backwards and being scattered forwards may even have polarization vectors pointing in the opposite direction from the vectors of the "true electrons". The scattered electrons, hence, decrease the

degree of longitudinal polarization of the electron beam. One can calculate the value of depolarization theoretically (57-59). The calculations are best checked by additional experiments, for instance, by varying the source or the source backing thickness. In the source, polarization usually occurs either by a large-angle single scattering or by small-angle multiple scattering. Calculations (58, 59) show that these two effects give rise to terms of the same order of magnitude.

Experimental investigation of the influence of the source thickness and backing thickness on the measured value of the polarization showed negligible effects, especially when the backing material was of mylar having a low average value of Z. The depolarization due to scattering from walls, from the foil and source holders, and from the plates, of the polarization transformer is much more difficult to study. Theoretical calculations are nearly impossible. In our case, these parts cause a negligibly small correction which is well within the experimental error. This is due to the use of alkathene pipes for making the scattering chamber and the connecting links. Moreover, the symmetrical nature of the Wien-filter arrangement causes the effect of equal magnitude for both the detectors.

V-3. Instrumental Asymmetry: And Finite Angle Correction:-

In practice, a number of essential precautions were taken in order to ensure the reliability of the results to within about ± 5 to 8%.

(a) The source used in the experiments was thin, about 3 to 4 mg/sq.cm^2 and uniformly spread over the backing material of low Z in order to minimize depolarization and back scattering.

(b) The energy or momentum selector and the slit system were symmetric and spurious scattering of electrons was negligible. By the second collimating slit these were prevented from being incident on the scattering foil.

(c) A thin gold $\leq$ 1 mg/cm^2 foil was employed as the target. The position of the scattering foil vis-a-vis the beam size and the counter positions, is crucial. In early experiments, foils were placed at 45^o to the beam, and the intensities L and R were then determined. It turned out, however, that such an arrangement is extremely inconvenient. Multiply scattered electrons may mask the polarization effect completely(36). The foil in the present experiment was placed at 60^o to the beam, and the scattered electrons were observed at azimuthal angles 90^o and 270^o.

(d) Two methods allow the determination of

instrumental asymmetries (43, 60). The first more common one, is to replace the gold foil by an aluminium foil as the value $S(\theta)$ is small for aluminium. In the second method one uses the fact that even for gold $S(\theta)$ is very small at scattering angles around 30°. Thus, two additional counters at small scattering angles around 30° are employed to get the data necessary for this correction. Unfortunately, these measurements eliminate only some of the instrumental asymmetries. Even small misalignments of the electron beam with respect to the symmetry axis of the system can introduce large errors.

Basically there are two ways in which error creeps in; (A) one in which the effective distances of the two counters from a particular scattering centre on the foil are different, and (B) the scattering angle may be unequal for the counters with respect to this scattering centre. These errors are discussed, in detail, below:

The actual mean direction of the incident beam may not be known. It was, therefore, not possible to know the exact scattering angle θ, accurately. Errors in angle θ will be caused by (i) the non-coincidence of the scattering centre S_c (see fig on p.80) with the geometrical centre SCC, (ii) the possible imperfect alignment of the mean beam direction with the 0°-180° direction of the scattering chamber and (iii) the finite

angle of convergence of the beam incident on the target. The solid angle $d\omega$ will also be in error due to (i). However, the exact knowledge of θ was not essential, provided scattering measurements on both sides of the incident beam at angles $\theta_1 (= \theta \pm \delta\theta)$ and $\theta_2 (= \theta \mp \delta\theta)$ were made and the total angle $2\theta = \theta_1 + \theta_2$ measured accurately.

In such measurements, the errors $\frac{dN}{N}$ in the number of the scattered electrons due to small errors $\pm \delta\theta (\sim 0.5^\circ)$ in the angle are eliminated, provided (i) the position and the cross section of the beam have remained the same during the scattering runs on the two sides and (ii) the relative error $\frac{\delta\theta}{\theta}$ was small.

These errors are derived below:

(a) <u>Error in the solid angle</u>:

This is caused by the error in the distance between the scattering centre and the $d\omega$ selecting aperature. For a perfect geometry, the solid angle $d\omega = \frac{\Delta S}{R_0^2}$ where, S = area of the aperture, and R_0 = distance of SSC from the centre of the aperture.

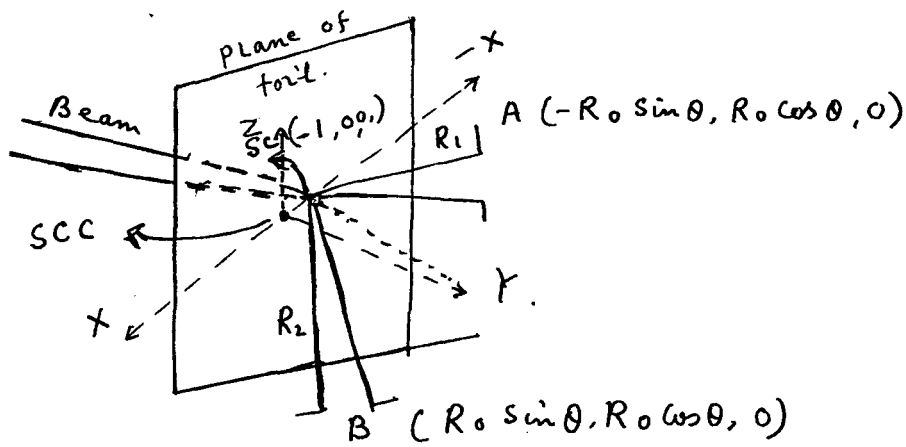

with the origin at SSC, the co-ordinates of the scattering centre SC are $(-x, 0, 0)$ with $x = 0.1$ cm; and those of the centres of the aperture at A and B are $(-R_0 \sin\theta, R_0 \cos\theta, 0)$ and $(R_0 \sin\theta, R_0 \cos\theta, 0)$ respectively. Distance of A from SC = R_1

$$R_1^2 = \left[-R_0 \sin\theta - (-x)\right]^2 + R_0^2 \cos^2\theta$$

$$= R_0^2 + x^2 - 2x R_0 \sin\theta$$

$$\frac{R_1^2 - R_0^2}{R_0^2} = \frac{\Delta(R_0^2)}{R_0^2} = \frac{x^2 - 2x R_0 \sin\theta}{R_0^2}$$

Similarly the error $\frac{\Delta R_0^2}{R_0^2}$ when the aperture is at B is $\frac{x^2 + 2x R_0 \sin\theta}{R_0^2}$. The nett error in the average value is negligible. The distance R_0 was therefore measured from SSC on both sides of the incident beam.

(b) Error $\pm \delta\theta$ in the angle θ.

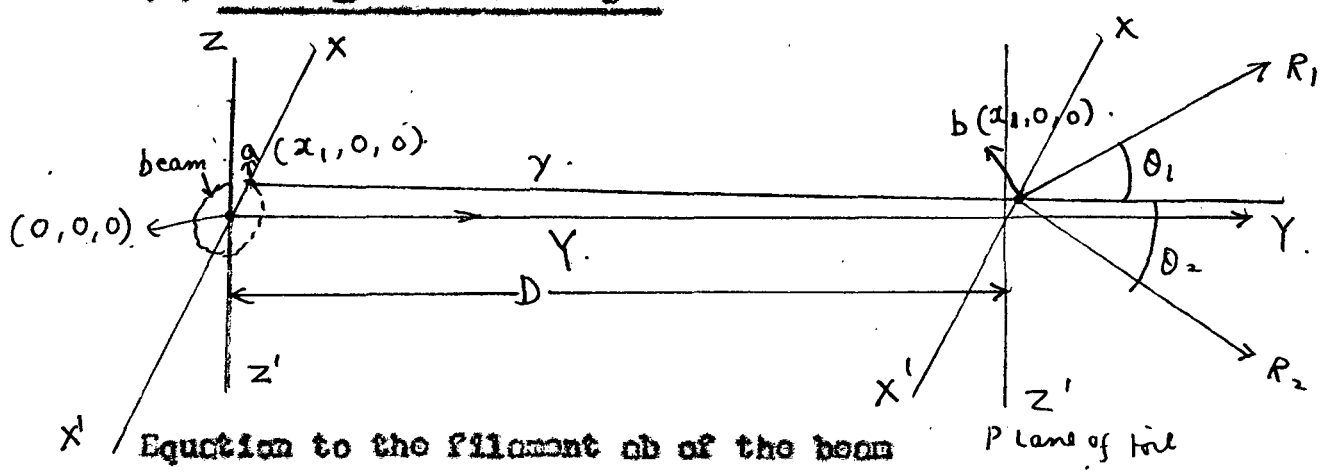

Equation to the filament ab of the beam

$$\frac{x - x_1}{l} = \frac{y - y_1}{m} = \frac{z - z_1}{n} = \gamma(-D)$$

i.e. $\frac{x_2 - x_1}{\ell} = \frac{D}{m} = \gamma$

The direction cosines of ab are

$$\ell = \frac{x_2 - x_1}{\gamma} \; ; \quad \text{and} \quad m = \frac{D}{\gamma} \sim 1 \; ; \quad n = 0$$

The direction cosines of R_1 are $(-\sin\theta, \cos\theta, 0)$ and of R_2 are $(\sin\theta, \cos\theta, 0)$, where $\theta = 60^\circ$ in the present case. The angle θ_1 is given in terms of angle θ by the expression

$$\cos\theta_1 = \frac{-(x_2 - x_1)\sin\theta}{D} + \cos\theta \quad \text{where } \theta_1 \sim \theta$$

After swinging the foil through the main beam by an angle

$$2\theta = \theta_1 + \theta_2 .$$

$$\cos\theta_2 = \frac{(x_2 - x_1)\sin\theta}{D} + \cos\theta .$$

Assuming that the number of electrons N, scattered along θ per unit solid angle is given by the Mott formula

$$N = \frac{K\cos^2\theta/2}{\sin^4\theta/2} = K\left[\frac{1}{\sin^4\theta/2} - \frac{1}{\sin^2\theta/2}\right]$$

$$N_1 = K\left[\frac{1}{\sin^4\theta_1/2} - \frac{1}{\sin^2\theta_1/2}\right] \text{ and } N_2 = K\left[\frac{1}{\sin^4\theta_2/2} - \frac{1}{\sin^2\theta_2/2}\right]$$

$$\sin^2\frac{\theta_1}{2} = \sin^2\frac{\theta}{2}\left[1 + p\right] \text{ where } p = \frac{(x_2 - x_1)\sin\theta}{2D\sin^2\theta/2}$$

then it can be shown that

$$N_1 + N_2 = 2N\left[1 - \frac{(x_2 - x_1)^2}{2D\sin^2\theta/2}\right].$$

the error $\frac{dN}{N}$ was small for an average

$$N = \frac{N_1 + N_2}{2}$$

Thus, the small errors in θ due to misalignment are cancelled if the average of two measurements, at $\theta_1 \simeq \theta_2 \simeq \theta$ is considered.

However, we were interested only in relative measurements which can be carried out with greater accuracy if the depolarization in the various sources to be used is small. In this case the uncertainties in the numerous corrections, such as apparatus asymmetry, beam misalignment etc. are not necessary to be known, if we have the same conditions of measurement for all sources. All that is necessary is that these are small and remain constant. The absolute value can then found from relative values.

V-4. Conclusions and Future Possibilities:

The helicity of beta particles has been measured in a few cases. We have not aimed at completeness of measurements so far as the present thesis is considered. However, the measurements reported have been very satisfactory in so far as these show the inherent possibilities of good results that can be obtained.

The following points bring out the salient features

of the performance of the equipment constructed by the author and the improved quality of the results as compared to those obtained with similar apparatus by other workers.

(1) The performance of the Wien-filter is quite satisfactory. The energy resolution as shown in fig (20) is slightly better than that reported by earlier workers. In the method of crossed fields, in the form we were able to employ it, the electrons are not focussed, and a high transmission can be achieved only at the expense of resolution with respect to energy. The effect of azimuthal asymmetry falls off slowly with increasing electron energy; the degree of polarisation of beta electrons, according to the theory, rises slowly with energy ($\sim$ v/c). The beta spectrum of heavy elements is a slowly decreasing function of electron energy, and finally, the angle of turning of the spin is also a slowly changing function. Therefore, the measurements of polarisation of beta electrons can be carried out with a wide spectrum of electron energies.

Thus, the main purpose of the crossed electric and magnetic fields in our experiments, which influenced the spectral composition of the electrons falling on the scatterer only slightly, was to turn the spin and achieve a high transmission.

(2) Intensity of incident electrons can be increased by using high activity sources, but this entails a thick

source resulting in depolarisation effects. The depolarisation correction becomes large and uncertain.

(3) At high energies, the variation of v/c becomes slow and the experiment using such electrons cannot be very accurate. For low energy electrons, the spectrum is not well defined, and the theoretical calculations are not reliable, especially the effect of screening on the Mott scattering is not yet very well understood. In our present work, we have used the theoretical calculations of Nelson and Pidds in which the screening effect has been considered. However, separate low energy electron scattering experiments are in progress in this laboratory to study the effect of a screened nucleus on the Mott scattering cross section.

(4) It is necessary that the scattering foils should be uniform and thin. This was done in the present experiment by vacuum deposition of gold on thin foils of cellophane and myler. If the foils are extremely thin, it was observed, however, that they rupture in vacuum. Too thin foils also increase in inaccuracy in the measurement of their masses and areas.

(5) We have used plastic pipes and materials in the scattering chamber and the associated equipment. This was found advantageous as spurious counts from walls and other matter were reduced.

(6) The overall accuracy of relative measurement is of the order of $\pm$ 5%, contribution to the errors coming mainly from the statistics of counting.

~~V-3~~. Such measurements can be improved in accuracy still further provided the signal to noise ratio can be enhanced. This is now possible with the recently introduced solid state detectors of electrons operable ar room temperature. Such experiments are now being planned in this laboratory using the Wien-filter designed by the author for polarisation transformation. It is then possible to study more accurately the following variations of the helicity of beta particles which are not yet understood properly.

(a) The energy dependence of the helicity of the beta particles from one given isotope has not yet been investigated in sufficient detail to allow a satisfactory comparison with theory, or a search for possible deviations, in allowed decays. From the measurements reported so far, enough data on a single decay are not available. Generally, the helicities agree well with a simple v/c dependence. However, a note of caution must be interjected. The results available at present are still very crude and considerable deviations from the behaviour predicted by a two-component V-A theory could exist without being noticed.

(b) All allowed and most forbidden decays show, within the rather wide limits of error, a complete polarisation ($P_\ell = \pm v/c$). Departures from the normal value $P_\ell = \pm v/c$ can occur if the electron spectrum deviates from the allowed shape; they can be due to partial cancellation of nuclear matrix elements, to contributions from higher forbidden transitions or to additional selection rules. Experimentally, such deviations have been observed in a number of decays(9-15), but more accurate and refined experiments are required to extract all the information desired for complete analysis of the decays.

(c) One can also test the validity of deviation from v/c depending on nuclear structure by making measurements of polarisation of a simple nucleus.

(d) The accuracy of our measurements is of the order of a few percent. If one can carry out such measurements under identical conditions for a greater number of isotopes of widely varying values of Z or A, the results can be very valuable. We have chosen the source of Tl^{204}, Tm^{170}, Sr^{90} and Cl^{36} having a variation of Z = 64. Measurements of a few percent accuracy are expected to provide reliable information on the dependence of polarisation on the value of Z or A of the emitting nucleus.

Such measurements are possible with our apparatus which removes the largest source of error in these experiments, viz. that of misalignment and intrinsic asymmetry of the instrument. Provided we get the isotopes of various Z in suitable quantities, a series of experiments of reasonably good accuracy can be completed.

REFERENCES

1. T.D. Lee and C.N. Yang, Phys.Rev.104, 254 (1956).
2. L.D. Landau, Nuclear Physics 3, 127 (1957).
3. T.D. Lee and C.N. Yang, Phys.Rev. 105, 1671 (1957).
4. A. Salam, Nuovo Cimento 5, 299 (1957).
5. Landau Soviet Physics JETP 5, 336 (1957).
6. R.P. Feynman and M. Gell Mann, Phys.Rev.109,193(1958).
7. E.C.G. Sudarshan and R.E. Marshak,Phys.Rev.109,1860(1958)
8. J.S. Geiger, G.T. Ewan et al, Phys.Rev.112, 1684 (1958).
9. R.O. Avakyan, V.E. Pushkin et al, Soviet Physics JETP, 14, 491 (1962)
10. W. Buhring and J. Heintze Z. Physik, 153, 237 (1958).
11. D.M. Harmsen and K. Holm Z. Physik, 166, 227 (1962).
12. J.D. Ullman, H. Frauenfelder, H.J. Lipkin, A. Rossi, Phys.Rev. 122, 536 (1961).
13. A. Ladage, Dissertation, University of Hamburg, 1961.
14. H. Wegner Z. Physik, 154, 533 (1959).
15. A.I. Alikhanov, Eliseev and Lyubimov, Soviet Physics, JETP 12, 414 (1961).
16. J. Heintz Z. Physik, 150, 134 (1958).
17. N.F. Mott and H.S.W. Massey, Theory of Atomic Collisions' Oxford University Press London, 1949, and H.A. Tolhoek, Revs.Modern Phys.28, 277 (1956).
18. A.M. Bincer, Phys.Rev. 107, 1434 (1957).
19. P. Lipnik et al, Nuclear Physics, 30, 312 (1962).
20. N. Sherman, Phys. Rev. 103, 1601 (1956), Phys.Rev.114, 1541 (1959).
21. Lin and Percus, Nuclear Physics, 45, 492 (1963).

22. H. Wegner, Z. Physik, 151, 252 (1958).

23. H. Bienlein, K. Güthner, Nuclear Instrument, 4, 79(1959).

24. B. Mühlschlegel and H. Koppe Z. Physik, 150, 474 (1958).

25. A.R. Brosi, A.I. Galonsky, B.H. Kettle, and H.B.Willard, Bull. Am. Physics Soc. 4, 76 (1959).

26. DE-Shalit, S. Kuperman et al, Phys.Rev.107, 1459(1957).

27. F.Gürsey, Phy.Rev.107, 1734 (1957).

28. L.J. Tassie, Phy.Rev. 107, 1452 (1957).

29. H.J. Lipkin, S. Kuperman, Phy.Rev.109, 223 (1958).

30. Alikhnow Eliseyav and Luibimov, Nuclear Physic, 7, 655 (1958).

31. V.A. Apalin, P. YE. Spivak, L.A. Mikaelyan, Nuclear Physics, 31, 657, 663 (1962).

32. L. Mikaelyan, G. Feisner et al, Nuclear Physic, 47, 328 (1963).

33. P.E. Spivak, L.A. Mikaelyan, Nuclear Physics, 23, 169 (1961).

34. A.I. Alikhnov, G.P. Eliseyev, Nuclear Phys.13, 541(1959).

35. S. Kuperman, Nuclear Physics, 28, 84 (1961).

36. H.A. Tolhoek, Revs. Modern Physics, 28, 277 (1956).

37. K.T. Bainbridge, Experimental Nuclear Physics (E.Segre ed) Vol. 1, Part V Wiley (1953).

38. H. Frauenfelder, R. Bobone, et al. Phys.Rev.106,386(1957)

39. H. Bienlein, H. Wegener, Z. Physik, 150, 80 (1958).

40. H. DE-Waard and O.J. Poppema Physica, 23, 597 (1957).

41. J.S. Greenberg, D.P. Malone, Phys.Rev.120,1393 (1960).

42. B.V. Thosar, C.V. Pant, V.G. Kulkarni, Phys. Letters 7, 52 (1963).

43. A.R. Brosi, A.I. Galonsky, B.H. Kettle, Nuclear Phys., 33, 353 (1962).

44. P.E. Cavanagh, J.F. Turner, Phil. Mag. 21, 1105 (1957).

45. N. Benczer - Koller, C.S. Wu, Phys.Rev. 109, 85 (1958)

46. P.E. Cavanagh, Proc.Roy.Soc.Lond, 246, 466 (1958).

47. A.I. Alikhnov, G.P. Eliseiv, Nuclear Physics, 5, 588 (1958).

48. Experimental Nuclear Physics E. Segre, Russian Translation, 1955, P.239-241, B.Rossi, K.Greisen.

49. P.E. Spivak, L.A. Mikelyan, Nuclear Phys. 20, 475 (1960).

50. R. Sosnowski, Z. Wilhelmi, Nuclear Phys, 26, 280 (1961)

51. V. Bargmann, L. Michel, V.L. Telegdi, Phys. Rev. Letters 2, 435 (1959).

52. T.K. Khoe, L.C. Teng, Argonne National Laboratory, Report ANLAD 69 (1962).

53. R.H. Good, Jr. Phys. Rev. 125, 2112 (1962).

54. J.H. Bartlett and R.E. Watson, Proc. Am. Acad. Arts. Sci. 74, 53 (1940).

55. Ferdin and Voelker, Lawrence Radiation Laboratory, Report Engineering Note, EE-304, Nov. 5, (1954).

56. S. Cuperman Nuclear Physics, 28, 84 (1961).

57. G. Passatore, Nuovo Cemento, 18, 532 (1960).

58. B. Mühlsehlegel Z. Physik, 155, 69 (1959).

59. B. Blake and B. Mühlsehlegel Z. Physik, 167, 584(1962).

60. L. Grodzins, Progress in Nuclear Physics, 7, 163 (1959).

61. D.F. Nelson and Pidds, Phys.Rev. 114, 728 (1959).

62. B.V. Geshkenbein and A.P. Rudik, Soviet Physics JETP 11, 1361 (1960).
